

RESEARCH ARTICLE

$\gamma\delta$ T cell IFN γ production is directly subverted by *Yersinia pseudotuberculosis* outer protein YopJ in mice and humans

Timothy H. Chu^{1,2}, Camille Khairallah^{1,2}, Jason Shieh³, Rhea Cho^{1,2}, Zhijuan Qiu^{1,2}, Yue Zhang^{1,2}, Onur Eskiocak⁴, David G. Thanassi^{1,2}, Mark H. Kaplan⁵, Semir Beyaz⁴, Vincent W. Yang³, James B. Bliska⁶, Brian S. Sheridan^{1,2*}

1 Department of Microbiology and Immunology, Renaissance School of Medicine, Stony Brook University, Stony Brook, New York, United States of America, **2** Center for Infectious Diseases, Renaissance School of Medicine, Stony Brook University, Stony Brook, New York, United States of America, **3** Department of Medicine, Renaissance School of Medicine, Stony Brook University, Stony Brook, New York, United States of America, **4** Cold Spring Harbor Laboratory, Cold Spring Harbor, New York, United States of America, **5** Department of Microbiology and Immunology, School of Medicine, Indiana University, Indianapolis, Indiana, United States of America, **6** Department of Microbiology and Immunology, Geisel School of Medicine, Dartmouth College, Dartmouth, New Hampshire, United States of America

* brian.sheridan@stonybrook.edu



OPEN ACCESS

Citation: Chu TH, Khairallah C, Shieh J, Cho R, Qiu Z, Zhang Y, et al. (2021) $\gamma\delta$ T cell IFN γ production is directly subverted by *Yersinia pseudotuberculosis* outer protein YopJ in mice and humans. PLoS Pathog 17(12): e1010103. <https://doi.org/10.1371/journal.ppat.1010103>

Editor: Denise M. Monack, Stanford University School of Medicine, UNITED STATES

Received: July 29, 2021

Accepted: November 9, 2021

Published: December 6, 2021

Copyright: © 2021 Chu et al. This is an open access article distributed under the terms of the [Creative Commons Attribution License](https://creativecommons.org/licenses/by/4.0/), which permits unrestricted use, distribution, and reproduction in any medium, provided the original author and source are credited.

Data Availability Statement: The RNA-seq datasets generated during this study are available at Bioproject accession number PRJNA742496 in the NCBI Bioproject database (<http://www.ncbi.nlm.nih.gov/bioproject/742496>).

Funding: This work was supported by The G. Harold and Leila Y. Mathers Foundation grant MF-1901-00210 (B.S.S.), the NIH grants T32 AI007539 (T.H.C.), R01 AI099222 (J.B.B.), K12 GM102778 (Z.Q.), and R01 AI141633 (D.G.T.), and funds provided by The Research Foundation for the State

Abstract

Yersinia pseudotuberculosis is a foodborne pathogen that subverts immune function by translocation of *Yersinia* outer protein (Yop) effectors into host cells. As adaptive $\gamma\delta$ T cells protect the intestinal mucosa from pathogen invasion, we assessed whether *Y. pseudotuberculosis* subverts these cells in mice and humans. Tracking Yop translocation revealed that the preferential delivery of Yop effectors directly into murine V γ 4 and human V δ 2⁺ T cells inhibited anti-microbial IFN γ production. Subversion was mediated by the adhesin YadA, injectisome component YopB, and translocated YopJ effector. A broad anti-pathogen gene signature and STAT4 phosphorylation levels were inhibited by translocated YopJ. Thus, *Y. pseudotuberculosis* attachment and translocation of YopJ directly into adaptive $\gamma\delta$ T cells is a major mechanism of immune subversion in mice and humans. This study uncovered a conserved *Y. pseudotuberculosis* pathway that subverts adaptive $\gamma\delta$ T cell function to promote pathogenicity.

Author summary

Unconventional $\gamma\delta$ T cells are a dynamic immune population important for mucosal protection of the intestine against invading pathogens. We determined that the foodborne pathogen *Y. pseudotuberculosis* preferentially targets an adaptive subset of these cells to subvert immune function. We found that direct injection of *Yersinia* outer proteins (Yop) into adaptive $\gamma\delta$ T cells inhibited their anti-pathogen functions. We screened all Yop effectors and identified YopJ as the sole effector to inhibit adaptive $\gamma\delta$ T cell production of IFN γ . We determined that adaptive $\gamma\delta$ T cell subversion occurred by limiting activation of the transcription factor STAT4. When we infected mice with *Y. pseudotuberculosis*

University of New York (B.S.S.) and Stony Brook University (B.S.S.). The funders had no role in study design, data collection and analysis, decision to publish, or preparation of the manuscript.

Competing interests: The authors have declared that no competing interests exist.

expressing an inactive YopJ, this enhanced the adaptive $\gamma\delta$ T cell response and led to greater cytokine production from this subset of cells to aid mouse recovery. This mechanism of immune evasion appears conserved in humans as direct injection of *Y. pseudotuberculosis* YopJ into human $\gamma\delta$ T cells inhibited cytokine production. This suggested to us that *Y. pseudotuberculosis* actively inhibits the adaptive $\gamma\delta$ T cell response through YopJ as a mechanism to evade immune surveillance at the site of pathogen invasion.

Introduction

Pathogens in the genus *Yersinia* include three species (*Y. pestis*, *Y. pseudotuberculosis*, and *Y. enterocolitica*) that can cause human disease. *Y. pseudotuberculosis* and *Y. enterocolitica* cause enteric infections [1,2] while *Y. pestis* is the causative agent of bubonic, septicemic, and pneumonic plague that has claimed over 200 million human lives [3,4]. Bubonic and septicemic plague is transmitted by blood sucking fleas while aerosols spread the pneumonic plague. Despite vaccine availability [5], and sensitivity to antibiotic treatment, pneumonic plague commonly results in fatality in part due to the rapid course of the infection [6].

Pathogenic *Yersinia spp.* harbor a virulence plasmid that encodes numerous virulence factors to subvert host immune responses, including IFN γ production [7–9]. Immune cell subversion requires *Yersinia* adherence to host cells through bacterial adhesins and translocation of *Yersinia* outer proteins (Yop) effectors into the host cell cytoplasm by a type III secretion system (T3SS). *Yersinia spp.* predominately target host phagocytes like macrophages, dendritic cells (DC), neutrophils, and B cells to subvert immune function during infection, but injection into other immune populations like conventional T cells has been reported, albeit to a lesser degree than their phagocytic counterparts [10–12]. *Yersinia* virulence factors include components of the T3SS (e.g., YopB) and translocated effectors (e.g., YopJ and YopH). YopB forms a pore in the host cell membrane necessary for translocation of Yop effectors [13,14]. Numerous Yop effectors translocate into host cells to inhibit immune responses and promote *Yersinia spp.* pathogenesis. One notable example is YopJ, an acetyl transferase and a possible cysteine protease that inhibits the mitogen-activated protein kinase (MAPK) pathway and tumor necrosis factor receptor-associated factor (TRAF) ubiquitination [15–19]. YopJ is the major Yop effector responsible for the induction of pyroptosis in macrophages during infection [20] and limits toll-like receptor 4 (TLR4) dependent signaling pathways [21]. While YopJ has no known direct effects on conventional T cell activation, YopP (a YopJ homolog in *Y. enterocolitica*) indirectly inhibits T cell priming via DC subversion [22]. YopH has been reported to have direct effects on conventional T cells *in vitro*. Transfection of a YopH expression plasmid into Jurkat or human T cells inhibited T cell receptor (TCR) signaling and promoted T cell apoptosis [23,24]. Additionally, stimulation of Jurkat cells with a YopH deficient *Y. pseudotuberculosis* restored T cell signaling and IL-2 production [25,26]. Even in this context, it is notable that many of the downstream targets in the $\alpha\beta$ TCR signaling pathway were inhibited at an excessively high (>50) multiplicity of infection (MOI) and *in vivo* relevance is unclear [23,26]. Thus, the role of direct subversion of T cell function, especially among unconventional T cells, by *Yersinia spp.* remains largely unexplored.

$\gamma\delta$ T cells make up a large proportion of lymphocytes at barrier surfaces and mucosal tissues including the intestines of mice and humans [27,28]. This is particularly pertinent to infections caused by *Y. pseudotuberculosis*, which has evolved to invade the intestinal barrier. The activity of $\gamma\delta$ T cells can be modulated by numerous cell-intrinsic and environmental factors like the $\gamma\delta$ TCR, cytokines, and co-stimulatory or inhibitory receptors [29]. For example, IL-12 and

IL-18 may promote IFN γ production from some $\gamma\delta$ T cell subsets whereas IL-1 β and IL-23 predominantly drive IL-17A production from other $\gamma\delta$ T cell subsets [30–35]. V γ 4V δ 1 (Garman nomenclature [36]) T cells have traditionally been considered an innate-like cell. However, our group recently characterized a long-lived CD27⁻ CD44^{hi} V γ 4V δ 1 T cell memory population in the context of foodborne *Listeria monocytogenes* infection [37,38]. While V γ 4 T cells are typically programmed for IL-17A production, this subset has the multifunctional capacity to produce both IL-17A and IFN γ [37]. Similar observations of IFN γ production were made in clonally expanded V γ 4 T cells in response to *Staphylococcus aureus* in the skin [39]. IFN γ activates macrophages to kill intracellular pathogens or phagocytosed bacteria and induces chemokines that attract immune cells to the site of infection. IFN γ is a critical cytokine in protection from *Y. enterocolitica* infection [2,40], *Y. pestis* intranasal challenge [41], and associated with protection from *Y. pseudotuberculosis* [42]. Interestingly, IFN γ but not IL-17A production from type-3 innate lymphoid cells is critical for the control of foodborne *Y. enterocolitica* infection [43]. As such, unconventional T cells like V γ 4 T cells that are ideally placed to provide protection against pathogen invasion at mucosal sites may be particularly relevant to *Yersinia* infections that invade mucosal barriers of the lungs (pneumonic *Y. pestis*) and gut (*Y. pseudotuberculosis* and *Y. enterocolitica*).

Despite a foundational understanding of *Yersinia* pathogenesis, physiologically robust evidence linking *Yersinia* pathogenesis to direct subversion of T cell function is lacking. Here, we uncovered a novel YopJ-dependent immunomodulatory pathway used by *Y. pseudotuberculosis* to directly subvert a murine V γ 4V δ 1 anti-microbial response to aid *Y. pseudotuberculosis* pathogenesis. *Y. pseudotuberculosis* also directly subverted a human V δ 2⁺ T cell IFN γ response, suggesting that this pathway may function similarly in human infection to aid *Y. pseudotuberculosis* pathogenesis.

Results

Viable *Y. pseudotuberculosis* inhibits IFN γ production by adaptive $\gamma\delta$ T cells in a YopB- and YadA-dependent manner

Initial experiments were carried out to determine if *Y. pseudotuberculosis* inhibits adaptive $\gamma\delta$ T cell function *ex vivo*. To overcome the extremely low number of V γ 4 T cells in gut-associated lymphoid tissues of naïve specific pathogen free (SPF) mice, a previously established *in vivo* methodology was utilized to generate a sizable population of adaptive V γ 4 T cells for *in vitro* manipulation. As such, naïve Balb/c mice were exposed to foodborne *L. monocytogenes* and MLN enriched in adaptive $\gamma\delta$ T cells were isolated 9 days after infection [37], several days after mice typically clear *L. monocytogenes* [44]. MLN single cell suspensions were infected directly *ex vivo* with heat-killed or live wild-type (WT) *Y. pseudotuberculosis* (Yptb) 32777 (Table 1) at a multiplicity of infection (MOI) of 10 for 2 hours. Antibiotics were then added to prevent overgrowth of the live bacteria, and the cultures were incubated an additional 22 hours. Flow cytometry in conjunction with intracellular cytokine staining was used to assess IFN γ production from V γ 1.1/2⁻ CD44^{hi} CD27⁻ $\gamma\delta$ T cells (identifying the adaptive V γ 4 T cell subset [37,38]). Heat-killed *Y. pseudotuberculosis* elicited a significantly higher IFN γ response from adaptive V γ 4 T cells than was detectable after stimulation with live *Y. pseudotuberculosis* (Fig 1A). This observation suggests that live *Y. pseudotuberculosis* subverts adaptive V γ 4 T cell function. The virulence activity of *Y. pseudotuberculosis* relies substantially on its T3SS and translocation of Yop effectors into host cells. To determine if the T3SS is required for live *Y. pseudotuberculosis* inhibition of $\gamma\delta$ T cell function, MLN single cell suspensions were infected with WT *Y. pseudotuberculosis* or *Y. pseudotuberculosis* that were unable to translocate Yop effectors (Δ YopB) or lacked the virulence plasmid that encodes the T3SS (32777c) (Table 1)

Table 1. *Y. pseudotuberculosis* strains and mutants used in this study.

<i>Y. pseudotuberculosis</i>	Notation	Relevant Characteristics	References
32777	WT	<i>Yptb</i> wild-type serogroup O:1 strain	[47]
32777c	WT2777c	Virulence pYV-cured derivative of 32777 that lacks the T3SS	[47]
32777 YopJ ^{C172A}	YopJ ^{C172A}	Catalytically inactive YopJ	[45]
32777 YopH ^{R409A}	YopH ^{R409A}	Catalytically inactive YopH	[45,48,49]
32777 Δ YopB	Δ YopB	Deletion of YopB	[45,46]
32777 YopE ^{R144A}	YopE ^{R144A}	Catalytically inactive YopE	[45]
32777 YopT ^{C139A}	YopT ^{C139A}	Catalytically inactive YopT	[45]
32777 Δ YopM	Δ YopM	Deletion of YopM	[50]
32777 Δ YpkA	Δ YpkA	Deletion of YpkA	[51]
32777 Δ YopK	Δ YopK	Frameshift mutation in YopK	[52]
32777 YopE/ β -lac	WT <i>Yptb</i> - β la	YopE TME-1 β -lactamase fusion protein	[53–55]
32777 Δ YopB YopE/ β -lac	Δ YopB <i>Yptb</i> - β la	Deletion of YopB in the YopE/ β -lac	[53–55]
IP2666	WT	<i>Yptb</i> wild-type serogroup O:3 strain	[47]
IP40	Δ YopB	IP2666 yopB40 (a stop codon at codon 8 of YopB followed by a frameshift)	[56]
IP2666 Δ Inv	Δ Inv	Deletion of adhesin and invasin	[12,57]
IP2666 Δ YadA	Δ YadA	Deletion of adhesin and YadA	[12,57]
IP2666 Δ Inv Δ YadA	Δ Inv Δ YadA	Deletion of adhesin, invasion, and YadA	[12,57]
IP40 Δ Inv Δ YadA	Δ YopB Δ Inv Δ YadA	Deletion of invasion and YadA in IP40 and pMMB207 mCherry	[12,57]

<https://doi.org/10.1371/journal.ppat.1010103.t001>

[45–47]. $\gamma\delta$ T cell function was assessed 24 hours later as described above. Stimulation with live *Y. pseudotuberculosis* strains Δ YopB or 32777c restored the IFN γ response of V γ 1.1/2⁺ CD44^{hi} CD27⁺ $\gamma\delta$ T cells (Fig 1B), similar to levels seen after stimulation with heat-killed WT *Y. pseudotuberculosis* (Fig 1A). These data indicate that *Y. pseudotuberculosis* inhibits IFN γ production by V γ 4 T cells in a manner that requires the T3SS and translocation of Yop effectors.

Y. pseudotuberculosis adheres to host cells with the bacterial adhesins invasin (Inv) and YadA to translocate effectors through the T3SS [58–60]. For *Y. enterocolitica*, both Inv and YadA bind β_1 -integrin either directly or indirectly through the extracellular matrix, respectively [61]. Additionally, β_1 -integrin expressed on host cells is a known adhesion target for *Y. pseudotuberculosis* [60,62]. To evaluate the role of these adhesins in the inhibition of $\gamma\delta$ T cell function, live *Y. pseudotuberculosis* with a deletion of Inv (Δ Inv), YadA (Δ YadA), or both (Δ Inv Δ YadA) (Table 1) were utilized to infect MLN cell suspensions. V γ 1.1/2⁺ CD44^{hi} CD27⁺ $\gamma\delta$ T cells stimulated with Δ Inv bacteria produced only minimal IFN γ , comparable to unstimulated cells or cells stimulated with WT (Fig 1C). In contrast, Δ YadA or Δ Inv Δ YadA stimulation led to partial restoration of IFN γ production, and stimulation with Δ YopB or Δ YopB Δ Inv Δ YadA bacteria led to full restoration of IFN γ production (Fig 1C). Thus, YadA but not Inv contributes to translocation dependent inhibition of IFN γ production by V γ 4 T cells.

Translocation of Yop effectors into adaptive $\gamma\delta$ T cells by *Y. pseudotuberculosis* is associated with IFN γ inhibition

To determine if *Y. pseudotuberculosis* can translocate Yop effectors into adaptive V γ 4 T cells, a WT strain expressing a YopE- β -lactamase fusion protein (*Yptb*- β la) in conjunction with a FRET-based β -lactamase reporter assay was used [63]. YopE translocation into target cells can be readily assessed by a change in fluorescence using flow cytometry. Thus, translocation of the YopE- β -lactamase fusion protein reports Yop effector translocation by emission in the blue range (Yop⁺) or lack thereof by emission in the green range (Yop⁻) [10,64,65]. A YopB

translocation (Fig 2A). Yop translocation into $V\gamma 1.1/2^- CD44^{hi} CD27^- \gamma\delta$ T cells was comparable to known DC and macrophage targets (Fig 2A). Additionally, Yop translocation was more efficient into $V\gamma 1.1/2^- CD44^{hi} CD27^- \gamma\delta$ T cells than CD4 or CD8 T cells (Fig 2A). *Y. pseudotuberculosis* also preferentially targeted $V\gamma 1.1/2^- CD44^{hi} CD27^- \gamma\delta$ T cells over $CD44^- \gamma\delta$ T cells and activated phenotype CD4 or CD8 T cells for Yop translocation (S1C Fig). YadA and Inv promote *Yersinia* adherence by direct or indirect interactions with the β_1 -integrin [66–69]. Analysis of β_1 -integrin expression on $V\gamma 1.1/2^- CD44^{hi} CD27^- \gamma\delta$ T cells, CD4 T cells, and CD8 T cell revealed that most $V\gamma 1.1/2^- CD44^{hi} CD27^- \gamma\delta$ T cells expressed the β_1 -integrin (S2A Fig). In contrast, most conventional CD4 and CD8 T cells did not express the β_1 -integrin. In addition, use of the WT *Yptb*- β la reporter for Yop translocation demonstrated that Yop translocation was associated with higher β_1 -integrin expression among $\gamma\delta$ T cells (S2B Fig). Thus, *Y. pseudotuberculosis* selectively targets adaptive $\gamma\delta$ T cells for Yop translocation among a diverse group of immune populations assessed in an *ex vivo* culture system.

As adaptive $V\gamma 4$ T cells were directly targeted with Yop effector translocation, WT *Yptb*- β la was utilized to determine whether $V\gamma 1.1/2^- CD44^{hi} CD27^- \gamma\delta$ T cells that contained Yop effectors were functionally impaired. An MOI of 1 was used as it provided similarly sized populations of $V\gamma 1.1/2^- CD44^{hi} CD27^- \gamma\delta$ T cells that did or did not contain translocated effectors from the same culture conditions (S1B Fig). Among WT *Yptb*- β la stimulated cells, $Yop^+ V\gamma 1.1/2^- CD44^{hi} CD27^- \gamma\delta$ T cells had reduced IFN γ production as compared to their Yop^- counterparts (Fig 2B). To extend these results, the ability of *Y. pseudotuberculosis* to translocate Yop effectors into human $\gamma\delta$ T cells and inhibit IFN γ production was assessed in peripheral blood mononuclear cells (PBMC) cultures stimulated with the WT *Yptb*- β la reporter. Approximately 8% of human $V\delta 2^+$ T cells were Yop^+ and these cells had significantly reduced IFN γ production as compared to the Yop^- counterparts (Fig 2C and 2D). These data indicate that *Y. pseudotuberculosis* is capable of translocating Yop effectors into $\gamma\delta$ T cell subsets and inhibiting IFN γ production in mice and humans.

YopJ is necessary for *Y. pseudotuberculosis* to inhibit IFN γ production in adaptive $\gamma\delta$ T cells

As multiple effectors are translocated into target cells, a panel of *yop* mutant *Y. pseudotuberculosis* (Table 1) [45] was screened to determine if individual Yop effectors inhibit IFN γ production. Similar to the $\Delta YopB$ mutant, stimulation with a catalytically inactive YopJ ($YopJ^{C172A}$) mutant that lacks acetyl transferase activity, but not other mutant *Y. pseudotuberculosis*, restored IFN γ production in $V\gamma 1.1/2^- CD44^{hi} CD27^- \gamma\delta$ T cells (Fig 3A). The C172A mutation in YopJ prevents YopJ mediated inhibition of MAPK and NF- κ B signaling pathways by abolishing its serine and threonine acetylation activity [70]. A similar restoration of IFN γ production was observed in human $V\delta 2^+$ T cells from PBMC of healthy donors upon $YopJ^{C172A}$ *Y. pseudotuberculosis* stimulation (Fig 3B). Thus, the YopJ effector is responsible for inhibition of IFN γ production from murine $V\gamma 4$ and human $V\delta 2^+$ T cells.

YopJ inhibits expression of multiple genes, including *ifng*, in adaptive $\gamma\delta$ T cells

To uncover mechanisms by which YopJ inhibits IFN γ production, the transcriptome of cell sorter-purified $V\gamma 1.1/2^- CD44^{hi} CD27^- \gamma\delta$ T cells after WT or $YopJ^{C172A}$ *Y. pseudotuberculosis* stimulation of MLN cells was assessed by RNA-Seq. Principal component analysis revealed unique gene expression clustering, and approximately 900 genes were expressed at higher levels in the $YopJ^{C172A}$ stimulation as compared to WT *Y. pseudotuberculosis* (Fig 4A and 4B). These differentially expressed genes may include genes that are directly inhibited by YopJ

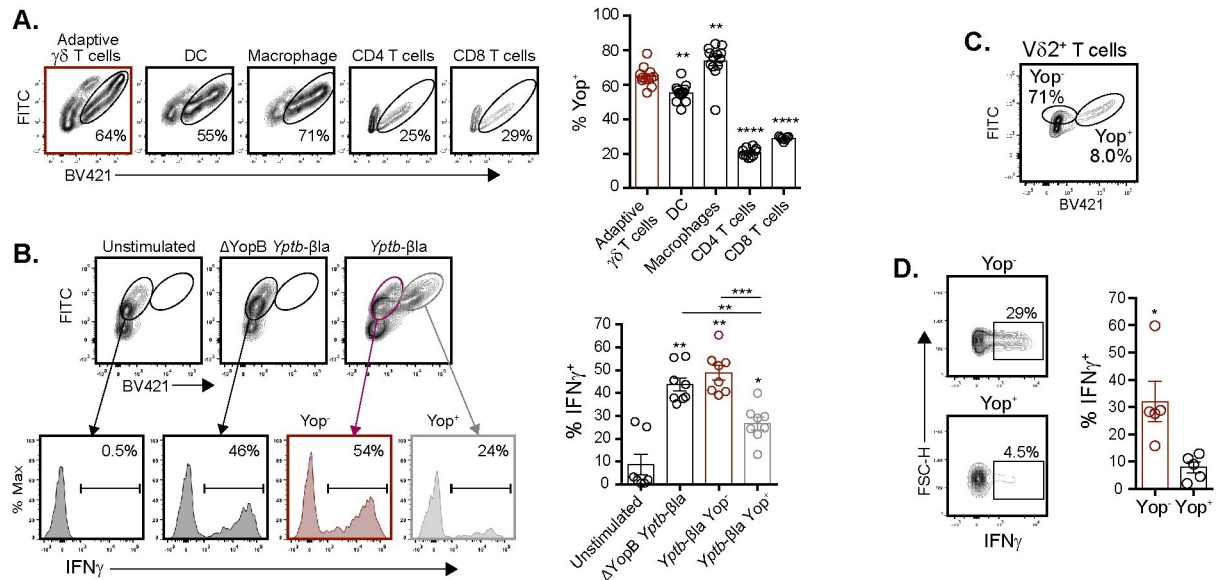


Fig 2. Direct translocation of Yop effectors inhibits the function of murine $V\gamma 4$ and human $V\delta 2^+$ T cells. MLN suspensions from *L. monocytogenes* infected mice (A and B) or human PBMC (C and D) were left unstimulated or stimulated with WT or $\Delta YopB$ *Yptb-βla* as indicated. Cells were loaded with CCF4-AM dye prior to stimulation to measure β -lactamase activity. FITC indicates CCF4-AM loaded cells without translocation (Yop^-) and BV421 indicates CCF4-AM loaded cells with Yop translocation (Yop^+). (A) Adaptive $\gamma\delta$ T cells ($V\gamma 1.1/2^-$ $CD44^{hi}$ $CD27^-$ $\gamma\delta$ T cells), DC ($CD11c^{hi}$ $MHCII^{hi}$), Macrophages ($F4/80^+$ $CD11b^+$), and CD4 and CD8 T cells were analyzed for Yop translocation 2 hours post stimulation at an MOI of 10. Representative contour plots are displayed. Yop translocation among the indicated populations is depicted as mean \pm SEM and is pooled from 2 experiments with a total of 4–8 mice per group. (B) Antibiotics were given 2 hours post-stimulation and brefeldin A was added for the last 5–6 hours of stimulation. $V\gamma 1.1/2^-$ $CD44^{hi}$ $CD27^-$ $\gamma\delta$ T cells were analyzed for Yop translocation and $IFN\gamma$ production 24 hours after stimulation. Representative contour plots and histograms are shown. $IFN\gamma$ production among the indicated populations is depicted as mean \pm SEM and is pooled from 3 experiments with a total of 8 mice per group. (C and D) Antibiotics were given 2 hours post-stimulation and brefeldin A was added for the last 5–6 hours of stimulation. $V\delta 2^+$ T cells were analyzed for Yop translocation and $IFN\gamma$ production post stimulation. Representative contour plots are displayed and $IFN\gamma$ production is quantified among Yop^+ or Yop^- $V\delta 2^+$ T cells. The graph depicts mean \pm SEM and is pooled from 3 experiments with 5 healthy donors per group. **** $p < 0.0001$, *** $p < 0.001$, ** $p < 0.01$, and * $p < 0.05$. An ordinary one-way ANOVA was used for (A), a repeated measures one-way ANOVA was used for (B), and a paired t-test was used for (D). Comparisons were performed to adaptive $\gamma\delta$ T cells in (A), to unstimulated or as depicted in figure in (B), and to Yop^+ in (C).

<https://doi.org/10.1371/journal.ppat.1010103.g002>

activity in $V\gamma 1.1/2^-$ $CD44^{hi}$ $CD27^-$ $\gamma\delta$ T cells or indirectly inhibited by YopJ activity in other cells such as DC or macrophages. To resolve this, the WT *Yptb-βla* reporter provided an opportunity to evaluate the molecular changes elicited by the activity of translocated Yop in adaptive $\gamma\delta$ T cells. The transcriptome of sort purified Yop^- and Yop^+ $V\gamma 1.1/2^-$ $CD44^{hi}$ $CD27^-$ $\gamma\delta$ T cells after WT *Yptb-βla* stimulation was assessed by RNA-Seq. Principal component analysis revealed unique gene expression clustering, and approximately 900 genes were more highly expressed in Yop^- vs Yop^+ $V\gamma 1.1/2^-$ $CD44^{hi}$ $CD27^-$ $\gamma\delta$ T cells after WT *Yptb-βla* stimulation (Fig 4C and 4D). Overlapping gene expression profiles from the two datasets were assessed to narrow the analysis to direct YopJ effects on $V\gamma 1.1/2^-$ $CD44^{hi}$ $CD27^-$ $\gamma\delta$ T cells. This comparison revealed 130 genes that were differentially expressed in both datasets, suggesting they are regulated directly by translocated YopJ in adaptive $V\gamma 4$ T cells (Fig 4E). These genes were categorized into different groups depending on their known functions. Some differentially expressed genes play a particular role in anti-infection functions (3.9%), stress sensing (1.6%), and lymphocyte activation/regulation (7.9%), genes that may be important for protective T cell responses (Fig 4E and 4F). Among these genes, $IFN\gamma$ was the single most significant differentially expressed gene suggesting it is a major target of direct YopJ-mediated inhibition of adaptive $\gamma\delta$ T cell function (Fig 4F). Differentially expressed genes among those that promote antimicrobial function included several that are important in augmenting type-1

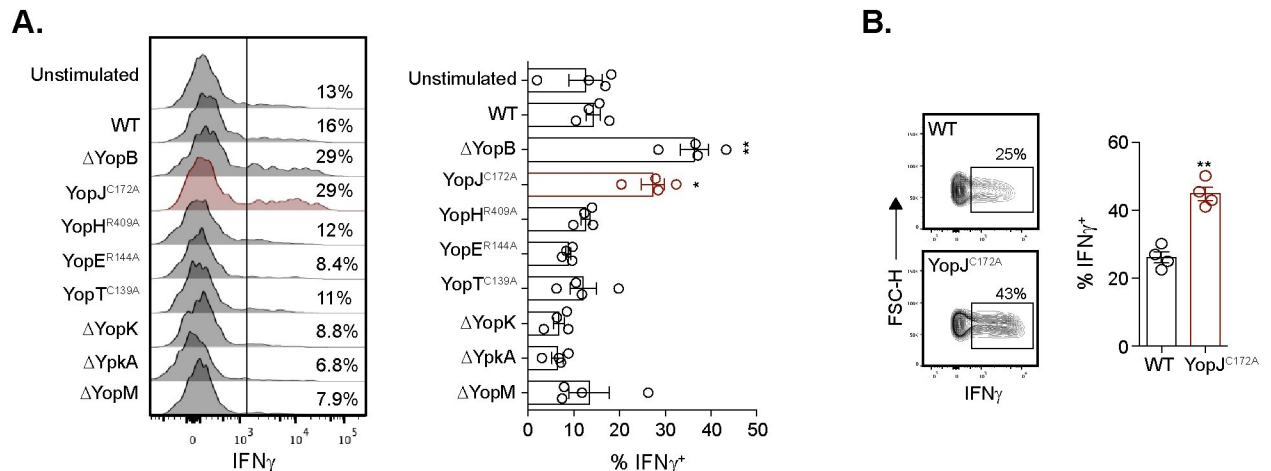


Fig 3. YopJ is necessary for inhibition of IFN γ production in murine V γ 4 and human V δ 2⁺ T cells. (A) MLN from *L. monocytogenes* infected mice were left unstimulated or stimulated with 10 MOI of the indicated *Y. pseudotuberculosis* for 24 hours. Antibiotics were given 2 hours post-stimulation and brefeldin A was added for the last 5–6 hours. V γ 1/2⁺ CD44^{hi} CD27⁻ $\gamma\delta$ T cells were analyzed for IFN γ post stimulation. Representative histograms are displayed. The graph depicts mean \pm SEM and represents at least two independent experiments with 2–4 mice per group. (B) Human PBMC were stimulated with 1 MOI of WT or YopJ^{C172A} *Y. pseudotuberculosis* for 24 hours. Antibiotics were given 2 hours post-stimulation. Brefeldin A was added for the last 5–6 hours of stimulation. V δ 2⁺ $\gamma\delta$ T cells were analyzed for IFN γ production post stimulation. Representative flow plots gated on V δ 2⁺ T cells are displayed. The graph depicts mean \pm SEM and is pooled from 2 experiments with 4 healthy donors. **p < 0.01 and *p < 0.05. A repeated measures one-way ANOVA was used for (A) and a paired t-test was used for (B). Experimental groups were compared to WT *Y. pseudotuberculosis*.

<https://doi.org/10.1371/journal.ppat.1010103.g003>

and -3 inflammation in T cells. For example, *Ptgs2* (encodes cyclooxygenase-2, COX2), *Nkg7* (natural killer cell granule protein 7), *Prf1* (perforin-1), and *Il17a* (IL-17A) appear to be regulated directly by translocated YopJ in adaptive V γ 4 T cells (Fig 4F) [71–73]. However, analysis of IL-17A protein after stimulation of MLN cell suspensions with YopJ^{C172A}, WT, and Δ YopB *Y. pseudotuberculosis* demonstrated that YopJ did not regulate IL-17A production from V γ 1.1/2⁻ CD44^{hi} CD27⁻ $\gamma\delta$ T cells (S4 Fig). Some of the observed differentially expressed genes are important in the activation status of T cells (e.g., *Il2ra*, *Ctla4*, and *Cd69*) and suggest that translocated YopJ may limit the activation of adaptive V γ 4 T cells. There was also a notable impact (48.0%) on genes associated with cell proliferation, metabolism and energy, mitosis and cell cycle, RNA/DNA processing, and ER/Golgi processing (Figs S3A and S3B and 4E), suggesting that YopJ influences the adaptive $\gamma\delta$ T cell transcriptional profile more broadly than just targeting the IFN γ pathway. Genes that were differentially expressed upon WT *Y. pseudotuberculosis* stimulation or among YopJ⁺ cells also suggest that many of the processes associated with immune responses and cellular activity were regulated by YopJ (S3C–S3E Fig). Collectively, YopJ appears to regulate the expression of many genes associated with T cell function in V γ 1.1/2⁻ CD44^{hi} CD27⁻ $\gamma\delta$ T cells, suggesting that adaptive V γ 4 T cells are broadly constrained in their immune functions by *Y. pseudotuberculosis*.

YopJ inhibits the IL-12p40-mediated STAT4 pathway in adaptive $\gamma\delta$ T cells

To gain potential mechanistic insights into YopJ inhibition of IFN γ production and other V γ 1.1/2⁻ CD44^{hi} CD27⁻ $\gamma\delta$ T cell functions, a motif discovery algorithm designed for regulatory element analysis was utilized to assess our RNA sequencing results [74]. Several transcription factor binding motifs related to IFN γ signaling were differentially expressed after YopJ^{C172A} *Y. pseudotuberculosis* but not WT *Y. pseudotuberculosis* stimulation including members of the E twenty-six (ETS)-domain family, Krüppel-like factor and specificity protein (KLF/SP) transcription factor gene family, and the interferon regulatory factors (IRF) family

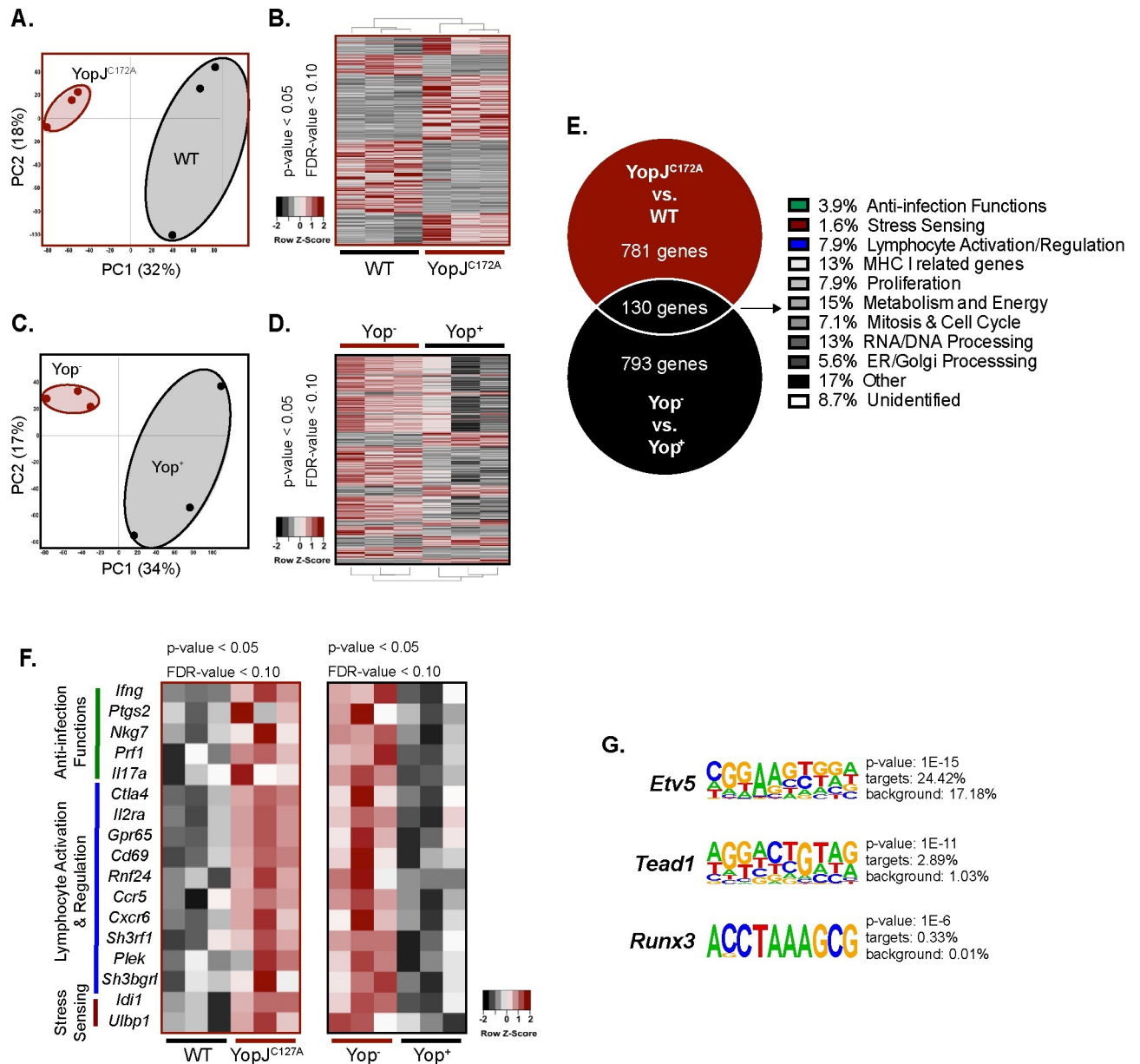


Fig 4. YopJ translocation leads to the inhibition of a broad anti-microbial gene response from V γ 4 T cells. (A and B) MLN suspensions from *L. monocytogenes* infected mice were stimulated with 10 MOI of WT or YopJ^{C172A} *Y. pseudotuberculosis* for 24 hours. Antibiotics were given 2 hours post-stimulation. Five hundred V γ 1.1/2⁺ CD44^{hi} CD27⁻ $\gamma\delta$ T cells from each stimulation were flow sorted and processed for RNA sequencing. (A) PCA plots are depicted for similarity of groups YopJ^{C172A} and WT *Y. pseudotuberculosis* stimulated V γ 1.1/2⁺ CD44^{hi} CD27⁻ $\gamma\delta$ T cells. (B) Heat maps are depicted for differentially expressed genes of YopJ^{C172A} or WT *Y. pseudotuberculosis* stimulated V γ 1.1/2⁺ CD44^{hi} CD27⁻ $\gamma\delta$ T cells. (C and D) MLN suspension from *L. monocytogenes* infected mice were stimulated with 1 MOI of WT *Yptb*- β la. Five hundred Yop⁺ or Yop⁻ V γ 1.1/2⁺ CD44^{hi} CD27⁻ $\gamma\delta$ T cells were flow sorted and processed for RNA sequencing. (C) PCA plots are depicted for similarity of Yop⁺ or Yop⁻ stimulated V γ 1.1/2⁺ CD44^{hi} CD27⁻ $\gamma\delta$ T cells. (D) Heat maps are depicted for differentially expressed genes of Yop⁻ or Yop⁺ stimulated V γ 1.1/2⁺ CD44^{hi} CD27⁻ $\gamma\delta$ T cells. (E-G) A Venn diagram of differentially expressed genes (higher) that overlapped between RNA sequencing analyses favoring YopJ^{C172A} *Y. pseudotuberculosis* stimulation or Yop⁻ cells is displayed. Shared genes were categorized by gene function. (F) The heat map highlights differentially expressed genes among V γ 1.1/2⁺ CD44^{hi} CD27⁻ $\gamma\delta$ T cells from the indicated stimulations and categories. (G) Homer motif analysis was performed on the RNA sequencing dataset. Motifs and associated genes to YopJ^{C172A} stimulated V γ 1.1/2⁺ CD44^{hi} CD27⁻ $\gamma\delta$ T cells are highlighted. Each experiment was performed with 3 biologic samples per group. Cutoffs for significant genes are $p < 0.05$ and $FDR < 0.10$.

<https://doi.org/10.1371/journal.ppat.1010103.g004>

of transcription factors (S5A Fig). IRF8 protein was validated after WT, Δ YopB, and YopJ^{C172A} *Y. pseudotuberculosis* stimulation. Indeed, a higher percentage of V γ 4 T cells expressed IRF8

protein after stimulation with Δ YopB compared to WT *Y. pseudotuberculosis* stimulation (S5B Fig). Stimulation with YopJ^{C172A} *Y. pseudotuberculosis* was also able to partially restore IRF8 levels to those seen after Δ YopB *Y. pseudotuberculosis* stimulation (S5B Fig). IRF8 was also impacted by IL-12p40 blockade, which signals through signal transducer and activator of transcription 4 (STAT4) (S5B Fig). Interestingly, a number of transcription factor binding motifs downstream of STAT4 signaling were enriched including *Etv5*, *Runx3*, and *Tead1* (Fig 4G) [75–78]. The RNAseq and homer motif analyses were also compared to an existing STAT4 ChIP-on-chip [79]. 7 genes identified from our main analyses (Figs 4F and 4G and S5B) were STAT4 target genes (S5C Fig). In summary, transcriptional profiling revealed a global subversion of anti-pathogen immune functions that may be associated with YopJ subversion of STAT4 activity.

IL-12 signaling leads to STAT4 phosphorylation and formation of STAT4-STAT4 homodimers that re-localize to the nucleus where they directly bind to the *Ifng* promoter to induce IFN γ expression [79–81]. To determine whether YopJ inhibits IFN γ production by interfering with the STAT4 pathway, STAT4 protein and phosphorylation were assessed by flow cytometry of MLN cells stimulated with *Y. pseudotuberculosis*. STAT4 phosphorylation was analyzed 6 hours after stimulation with WT, Δ YopB, or YopJ^{C172A} *Y. pseudotuberculosis*. Consistent with suppression of IFN γ production and the RNA-Seq analysis, WT *Y. pseudotuberculosis* significantly reduced the percentage of pSTAT4⁺ CD44^{hi} CD27⁻ $\gamma\delta$ T cells as compared to Δ YopB and YopJ^{C172A} *Y. pseudotuberculosis* (Fig 5A). However, STAT4 protein levels were the same in all three infection conditions (WT, Δ YopB, and YopJ^{C172A} *Y. pseudotuberculosis*) (Fig 5B). Flow cytometry antibodies for STAT4 protein were validated by comparing STAT4 from WT and STAT4 KO splenocytes (S5D Fig). These data suggest that STAT4 phosphorylation but not protein is decreased upon YopJ translocation. STAT4 phosphorylation was also evaluated using the *Yptb*- β la reporter system described above. Among CD44^{hi} CD27⁻ $\gamma\delta$ T cells, Yop⁻ cells had a higher percentage of pSTAT4⁺ cells compared to Yop⁺ cells suggesting intrinsic Yop mediated inhibition of STAT4 phosphorylation levels (Fig 5C). Additionally, as STAT4 phosphorylation is downstream of IL-12 signaling, an anti-IL-12/23p40 subunit antibody (anti-p40) was used to determine whether IL-12 signals in the environment regulated STAT4 phosphorylation after *Y. pseudotuberculosis* stimulation. Indeed, IL-12/23p40 neutralization abrogated STAT4 phosphorylation levels regardless of Yop translocation (Fig 5C). As IL-12/23p40 was required to elicit IFN γ production from adaptive V γ 4 T cells in the culture conditions, we assessed whether YopJ^{C172A} *Y. pseudotuberculosis* stimulation modulated IL-12p70. The concentration of IL-12p70 was comparable between WT and YopJ^{C172A} *Y. pseudotuberculosis* stimulated cultures (Fig 5D). Thus, changes in IL-12 were unlikely to contribute to adaptive V γ 4 T cell subversion *in vitro*. To understand the role of YopJ and IL-12 on V γ 1.1/2⁻ CD44^{hi} CD27⁻ $\gamma\delta$ T cells in a more simplified system, purified $\gamma\delta$ T cells were stimulated with YopJ^{C172A} *Y. pseudotuberculosis* in the presence of excessive IL-12p70. Adaptive V γ 4 T cells were unable to produce IFN γ in response to YopJ^{C172A} *Y. pseudotuberculosis* and IL-12p70 (S6A Fig). Finally, we assessed whether the addition of IL-12p70 could overcome the YopJ mediated inhibition of IFN γ production after WT *Y. pseudotuberculosis* stimulation. While a supraphysiologic level of IL-12p70 (50 ng/ml) was able to partially overcome YopJ mediated inhibition, lower levels of IL-12p70 addition (2 and 10 ng/ml) were unable to overcome YopJ mediated inhibition (S6B Fig). Importantly, these latter concentrations were orders of magnitude higher than those detected in our culture conditions. Thus, IL-12 is not sufficient to induce IFN γ production from adaptive V γ 4 T cells. Collectively, these results suggest that *Y. pseudotuberculosis* stimulation elicits IL-12 production to promote adaptive V γ 4 T cell IFN γ responses, and that YopJ translocation into adaptive V γ 4 T cells inhibits IL-12 mediated STAT4 phosphorylation.

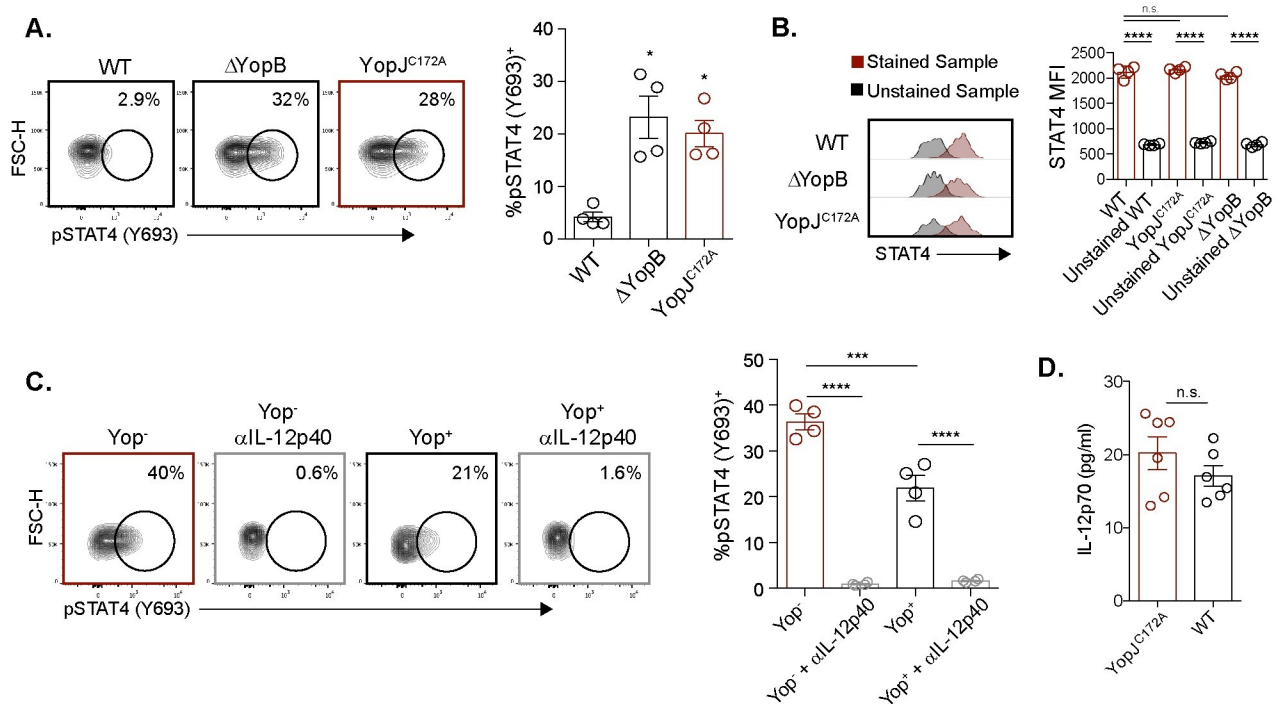


Fig 5. YopJ inhibits IL-12p40 mediated STAT4 phosphorylation. (A) MLN cell suspensions from *L. monocytogenes* infected mice were stimulated with 10 MOI of WT, YopJ^{C172A}, or Δ YopB *Y. pseudotuberculosis* for 6 hours. Antibiotics were given 2 hours after stimulation. V γ 1.1/2⁻ CD44^{hi} CD27⁻ $\gamma\delta$ T cells were analyzed for pSTAT4 after stimulation. Representative contour plots are displayed. The graph depicts mean \pm SEM and represents at least two independent experiments with 2–4 mice per group. (B) The same experimental setup was used as in (A), but V γ 1.1/2⁻ CD44^{hi} CD27⁻ $\gamma\delta$ T cells were analyzed for STAT4 protein after stimulation. Representative plots for mean fluorescent intensity (MFI) are displayed. The graph depicts mean \pm SEM and represents two independent experiments with 2 mice per group. (C) MLN suspensions from *L. monocytogenes* infected mice were either treated or untreated with IL-12/23p40 neutralizing antibody prior to stimulation with 1 MOI of WT *Yptb*- β la for 6 hours. Antibiotics were given 2 hours post-stimulation. V γ 1.1/2⁻ CD44^{hi} CD27⁻ $\gamma\delta$ T cells were analyzed for pSTAT4 after stimulation. Representative contour plots are displayed. The graph depicts mean \pm SEM and represents at least two independent experiments with 2–4 mice per group. (D) MLN cell suspensions from *L. monocytogenes* infected mice were stimulated with 10 MOI of WT or YopJ^{C172A} *Y. pseudotuberculosis* for 24 hours. Antibiotics were given 2 hours after stimulation. Supernatants were collected 24 hours post stimulation and IL-12p70 concentration was determined via ELISA. ****p < 0.0001, ***p < 0.001, **p < 0.01, and *p < 0.05. A repeated measures one-way ANOVA was used for (A–C). Comparisons were performed to WT *Y. pseudotuberculosis* in (A) and as depicted in (B–D).

<https://doi.org/10.1371/journal.ppat.1010103.g005>

Foodborne infection with YopJ^{C172A} *Y. pseudotuberculosis* induces IFN γ production in adaptive V γ 4 T cells

To determine whether YopJ subverts adaptive $\gamma\delta$ T cell function *in vivo*, foodborne infection with WT and YopJ^{C172A} *Y. pseudotuberculosis* was performed on naïve Balb/c mice. As YopJ^{C172A} *Y. pseudotuberculosis* is attenuated *in vivo* [82], a one log higher ($2\text{--}4 \times 10^8$ CFU) infection dose of YopJ^{C172A} *Y. pseudotuberculosis* was administered to normalize the internal bacteria burdens in the MLN between infection groups (S7A Fig). While mice infected with WT and YopJ^{C172A} *Y. pseudotuberculosis* lost a similar amount of weight, mice infected with YopJ^{C172A} *Y. pseudotuberculosis* recovered slightly faster (Fig 6A). MLN were isolated 9 days after infection to evaluate adaptive $\gamma\delta$ T cell function. Consistent with the *ex vivo* stimulation of *L. monocytogenes*-elicited V γ 4 T cells with *Y. pseudotuberculosis*, V γ 1.1/2⁻ CD44^{hi} CD27⁻ $\gamma\delta$ T cells from the MLN of YopJ^{C172A} *Y. pseudotuberculosis* infected mice displayed enhanced IFN γ production when stimulated *ex vivo* compared to their WT *Y. pseudotuberculosis* infected counterparts (Fig 6B and 6C). When the same infectious doses were used for both WT and YopJ^{C172A} *Y. pseudotuberculosis* (5×10^7 CFU), V γ 1.1/2⁻ CD44^{hi} CD27⁻ $\gamma\delta$ T cells from the MLN of YopJ^{C172A} *Y. pseudotuberculosis* infected mice also displayed enhanced IFN γ

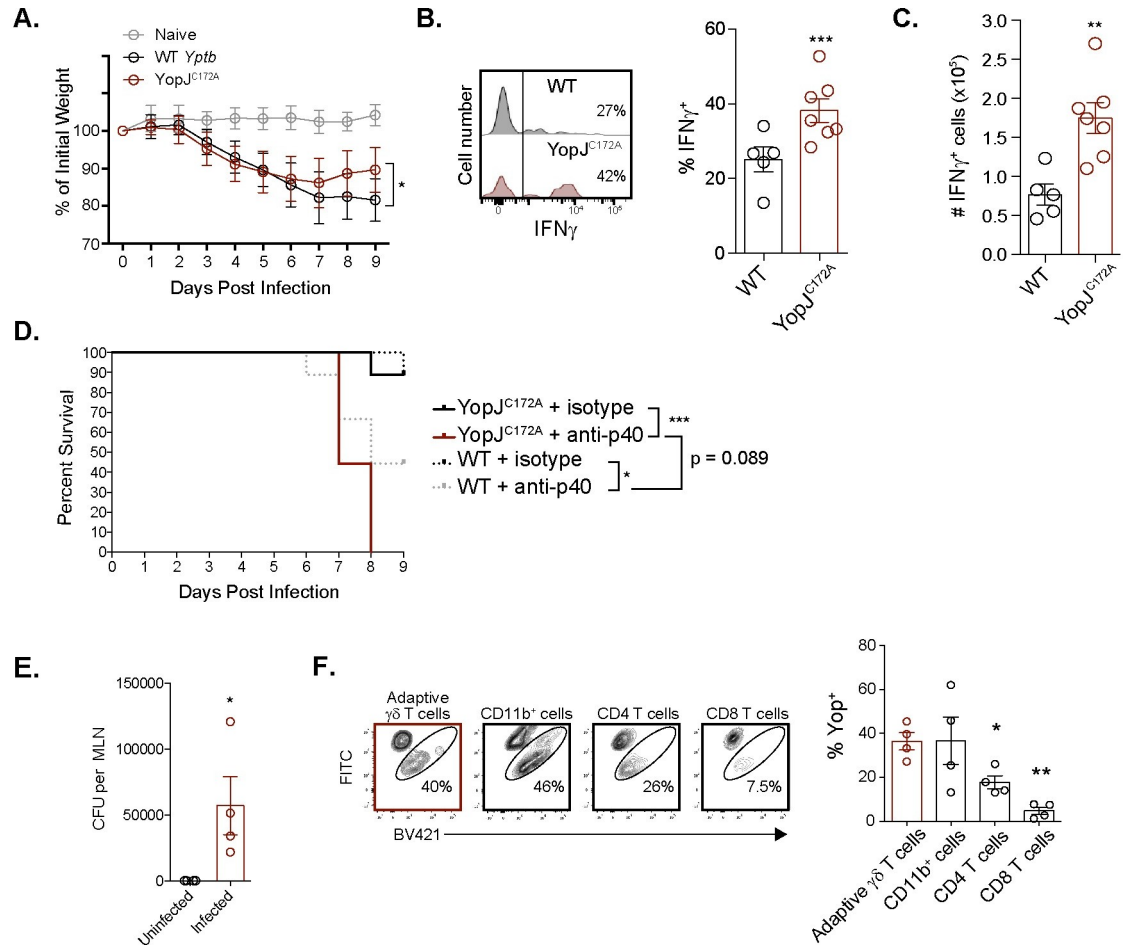


Fig 6. Foodborne YopJ^{C172A} *Y. pseudotuberculosis* infection elicits an IFN γ response from V γ 4 T cells. (A–E) Balb/c mice were foodborne infected with WT (2.4×10^7 CFU) or YopJ^{C172A} *Y. pseudotuberculosis* (2.4×10^8 CFU). (A) Mouse weight was assessed daily after infection. (B and C) Nine days post infection, MLN were processed into single cell suspensions and stimulated with PMA/ionomycin in the presence of brefeldin A for 4 hours. V γ 1.1/2⁺ CD44^{hi} CD27⁺ $\gamma\delta$ T cells were analyzed for IFN γ production. Representative histograms are displayed. Graphs represent mean \pm SEM and are pooled from 3 experiments with a total of 5–8 mice per group. (D) Mouse survival was assessed daily after infection. anti-IL-12p40 antibody was administered at 0.2 mg/mouse on 0, 2, 4, and 6 days post infection. A Kaplan-Meier survival plot is shown. Study endpoint was 9 days post infection. The data represent 2 independent experiments with a total of 9 mice per group. (E and F) Balb/c mice were foodborne infected with 2×10^9 CFU *L. monocytogenes* to elicit a V γ 1.1/2⁺ CD44^{hi} CD27⁺ $\gamma\delta$ T cell population *in vivo*. 30 days post infection, immunized mice were foodborne infected with WT *Yptb*- β la (2.4×10^9 CFU) or left uninfected. (E) CFU of WT *Yptb*- β la were enumerated in MLN 3 days post WT *Yptb*- β la infection. (F) Three days post foodborne WT *Yptb*- β la infection, V γ 1.1/2⁺ CD44^{hi} CD27⁺ $\gamma\delta$ T cells from the MLN were analyzed for Yop translocation using the CCF4-AM assay. Representative contour plots are shown. Yop translocation (Yop⁺) among the indicated populations is depicted as mean \pm SEM and is pooled from 2 experiments with a total of 4 mice per group. ***p < 0.001, **p < 0.01, and *p < 0.05. A repeated measures one-way ANOVA was used for (A and F) and an unpaired t-test was used for (B, C, and E). Experimental groups were compared to WT *Y. pseudotuberculosis* in (A–C), uninfected controls in (E), and V γ 1.1/2⁺ CD44^{hi} CD27⁺ $\gamma\delta$ T cells in (F). A logrank test was used for survival curves in (D).

<https://doi.org/10.1371/journal.ppat.1010103.g006>

production compared to their WT *Y. pseudotuberculosis* infected counterparts (S7B Fig). These experiments demonstrate that the increased IFN γ observed was not a result of a higher infectious dose nor of a higher bacteria burden at the time of analysis. As IL-12/23p40 was required for adaptive V γ 4 T cell IFN γ production *in vitro* (Fig 5), the impact of IL-12/23p40 was assessed *in vivo*. Naïve Balb/c mice were infected with WT or YopJ^{C172A} *Y. pseudotuberculosis* and treated with an IL-12/23p40 neutralizing antibody or isotype control. All YopJ^{C172A} *Y. pseudotuberculosis* infected mice treated with anti-IL-12/23p40 succumbed by day 8 post

infection (Fig 6D). This data suggests that IL-12 promotes the protective capacity of catalytically inactive YopJ. Similarly, IL-12 contributed to the protection of mice infected with WT *Y. pseudotuberculosis*. Serum was also collected on days 2, 4 and 6 after infection to assess circulating IL-12p70 levels. IL-12p70 was detectable 6 days after YopJ^{C172A} *Y. pseudotuberculosis* infection but was mostly below the limit of detection after WT *Y. pseudotuberculosis* infection (Fig 6E). Collectively, these data suggest that IL-12 is important in the protection of mice infected with WT or YopJ^{C172A} *Y. pseudotuberculosis*.

Foodborne infection with WT *Yptb-β1a* was performed to determine whether *Y. pseudotuberculosis* could target adaptive V γ 4 T cells with Yop translocation *in vivo*. Balb/c mice were foodborne infected with *L. monocytogenes* to elicit a population of V γ 1.1/2⁻ CD44^{hi} CD27⁻ $\gamma\delta$ T cells as described previously [37,83]. After a return to homeostasis at 30 days post *L. monocytogenes* infection, mice were foodborne infected with WT *Yptb-β1a*. *Y. pseudotuberculosis* burden was assessed in the MLN 3 days post foodborne infection to determine whether WT *Yptb-β1a* could establish a productive infection where V γ 4 T cells reside. Indeed, infected mice contained detectable *Y. pseudotuberculosis* in the MLN 3 days after foodborne infection (Fig 6F). Analysis of the translocation of Yop into V γ 1.1/2⁻ CD44^{hi} CD27⁻ $\gamma\delta$ T cells, myeloid cells (CD11b⁺), and CD4 and CD8 T cells was performed. Consistent with our *in vitro* observations, V γ 1.1/2⁻ CD44^{hi} CD27⁻ $\gamma\delta$ T cells and myeloid cells contained translocated Yop *in vivo* (Fig 6G). *Y. pseudotuberculosis* was relatively inefficient at Yop translocation into CD4 and CD8 T cells (Figs 6G and S7C). Collectively, these data show that foodborne YopJ^{C172A} *Y. pseudotuberculosis* infection of naïve mice elicits IFN γ production in adaptive $\gamma\delta$ T cells and that Yop can be translocated into adaptive V γ 4 T cells *in vivo*.

Discussion

In this study, we assessed the subversion of an adaptive subset of $\gamma\delta$ T cells specialized in the promotion of pathogen resistance at the intestinal mucosa through the production of anti-infective cytokines like IFN γ and IL-17A [37]. While limited evidence suggests that Yop effectors directly target T cells to subvert their function, we identified that the *Y. pseudotuberculosis* effector molecule YopJ directly inhibits IFN γ production from adaptive CD44^{hi} CD27⁻ $\gamma\delta$ T cells to subvert host immunity in mice. Additionally, we demonstrate that circulating human V δ 2⁺ T cells are similarly inhibited by direct translocation of YopJ, demonstrating that the direct targeting of $\gamma\delta$ T cells by *Y. pseudotuberculosis* to inhibit IFN γ production is a conserved pathway of immune evasion in humans. Thus, *Y. pseudotuberculosis* Yop effectors translocated into murine V γ 4 T cells and human V δ 2⁺ T cells directly subvert their anti-microbial functions and host immunity by limiting IFN γ production.

While *Yersinia* mediated inhibition of conventional T cells has been previously reported, studies have largely focused on the indirect subversion of T cells that is mediated by translocation of Yop effectors into myeloid cells [55,82]. For example, YopJ/P appears to primarily subvert conventional T cell function through indirect mechanisms associated with inhibiting DC [22,26]. On the contrary, the study of $\gamma\delta$ T cells in the context of *Y. pseudotuberculosis* infection has been primarily limited to the potential antigens that drive $\gamma\delta$ T cell recognition of infection [84–89].

After phagocytosis of pathogens, activated DC migrate to lymph nodes and present antigen to T cells. APC-derived IL-12 further shapes T cell responses by providing a critical signal during T cell activation [90]. Interestingly, *Y. pestis* can limit both the migratory capacity of DC and the production of IL-12 [91], and *Y. enterocolitica* can induce programmed death of DC and inhibit antigen presentation [22]. *Y. pseudotuberculosis* YopJ can also indirectly limit NK cell function by interfering with DC TLR4 signaling pathways and YopP in *Y. enterocolitica*

can limit NK cell function through STAT4 inhibition [21,92]. Given that IL-12 signaling promotes STAT4 phosphorylation and IFN γ production in $\gamma\delta$ T cells [29,93] and *Yersinia spp.* can inhibit DC, a potential extrinsic mechanism emerges for *Y. pseudotuberculosis* to inhibit $\gamma\delta$ T cell responses by suppressing DC functions. In line with these observations, IL-12p40 was critical for the induction of phospho-STAT4 in V γ 4 T cells after stimulation with *Y. pseudotuberculosis* in *in vitro* cultures. In contrast, *Y. pseudotuberculosis* and IL-12 were unable to directly elicit IFN γ production from a highly enriched population of *in vitro* expanded $\gamma\delta$ T cells suggesting that IL-12 is required but not sufficient for V γ 4 T cell IFN γ production. However, stimulation of MLN cell suspensions with Δ YopB or Yop^{C127A} *Y. pseudotuberculosis* elicited STAT4 phosphorylation among V γ 4 T cells suggesting that translocation of Yop effectors and YopJ in particular subverts V γ 4 T cell function. Tracking Yop translocation *in vitro* revealed that V γ 4 T cells that contain Yop had reduced pSTAT4 levels and inhibited IFN γ production. Importantly, V γ 4 T cells that did not contain Yop effectors from the same cultures expressed higher pSTAT4 levels and comparable IFN γ production as V γ 4 T cells stimulated with Δ YopB- β la *Yptb*. Additionally, IL-12 levels were comparable between cultures stimulated with WT and Yop^{C172A} *Y. pseudotuberculosis*. Collectively, these data suggest that functional impairment of V γ 4 T cells was mediated by direct translocation of YopJ into V γ 4 T cells and cell intrinsic mechanisms *in vitro*.

The YopJ effector family has been increasingly described by their acetyltransferase function on serine, threonine, and lysine amino acid residues [19,94]. Serine and threonine are common targets of phosphorylation to propagate signaling cascades or elicit functional consequences. For example, phosphorylation of STAT4 leads to dimerization and transport to the nucleus to promote transcription of STAT4 target genes. Acetylation of these target residues may inhibit phosphorylation and downstream signaling events [70]. Thus, a potential mechanism of YopJ subversion of V γ 4 T cells is through acetylation of STAT4 to inhibit the phosphorylation or dimerization of STAT4. Other potential targets of YopJ acetyltransferase activity are the IL-12R and Janus kinases upstream of STAT4 activation. YopJ has also been reported to have cysteine protease, lysine acetyltransferase, ubiquitin-like protein protease, and deubiquitinase activity that may provide other potential avenues for YopJ to modulate the function of V γ 4 T cells through STAT4 [94–96].

An important aspect of *Y. pseudotuberculosis* pathogenesis unveiled by this work is the preferential targeting of a specialized subset of $\gamma\delta$ T cells for delivery of inhibitory Yop effector molecules. *Y. pseudotuberculosis* injected Yop effectors into adaptive $\gamma\delta$ T cells in a similar proportion as macrophages and DC and to a much greater extent than conventional CD4 or CD8 T cells. Of note, *Y. pseudotuberculosis* has been reported to translocate Yop effectors more efficiently into T_{reg} cells than conventional CD4 T cells at high MOI to modulate their function [65]. The preferential targeting of V γ 4 T cells in this system is associated with expression of the β_1 -integrin by adaptive V γ 4 T cells. Additionally, the majority of adaptive V γ 4 T cells are anatomically segregated from conventional T cells in the paracortex by their localization in the interfollicular and medullary areas of the gut draining lymph nodes [38]. The distinct localization of adaptive V γ 4 T cells may facilitate interactions with *Y. pseudotuberculosis* *in vivo*. Loss of the adhesin YadA but not Inv abrogated YopJ mediated $\gamma\delta$ T cell inhibition, suggesting that *Y. pseudotuberculosis* utilizes YadA to target adaptive $\gamma\delta$ T cells for Yop translocation, consistent with previous studies suggesting that the adhesin Inv is largely dispensable for *Y. enterocolitica* virulence [61,97]. Interestingly, this appears distinct from the targeting of conventional CD4 T cells that relies on Inv and is enhanced in the absence of YadA [11,65].

While our data demonstrates that STAT4 phosphorylation is inhibited by YopJ, our RNA-Seq analysis suggests that other targets may also be affected. One of YopJ's known targets is the MAPK family of proteins that can have broad effects on cell proliferation, differentiation,

survival, and apoptosis [18]. The MAPK pathway in CD4 T cells and NK cells may also promote STAT4 activity and downstream IFN γ mRNA stabilization, respectively [98,99]. Our data demonstrate a broad impact of YopJ on adaptive $\gamma\delta$ T cell proliferation, metabolism, cell cycle, RNA/DNA processing, and ER/Golgi processing gene expression networks. These pathways may be regulated by MAPK family member activity [100–105]. Homer motif analysis identified other potential means by which YopJ may regulate IFN γ production. For example, Ets-1 is a T-bet cofactor and necessary for Th1 IFN γ responses [106]. Increases in ETS-domain family of transcription factor motifs were associated with type 3 innate lymphoid cells (ILC3) but not Th17 cells [107], which may suggest that one of the potential mechanisms of YopJ mediated inhibition may target conserved pathways in unconventional lymphocyte populations. Many NK cell receptors are also expressed on $\gamma\delta$ T cells and may facilitate TCR independent effector functions [108–110]. In line with this, our profiling demonstrates that YopJ limits gene expression of *Nkg7*, which has recently been reported to promote cytotoxic granule release and inflammation during infection and cancer [72], and *Prf1*, which encodes the pore forming molecule perforin necessary to deliver lytic machinery into target cells [111]. Finally, interactions with *Y. pseudotuberculosis* YopJ led to the upregulation of *Ulbp1*, which encodes a stress-induced NKG2D ligand, and *Idi1*, which encodes an enzyme in the mevalonate pathway. As human $\gamma\delta$ T cells respond to phospho-antigens derived from the non-mevalonate pathway in bacteria and mammalian mevalonate pathway in humans [112], this may limit the removal of translocated cells through NK or $\gamma\delta$ T cell sensing mechanisms and suggests a broad mechanism to subvert human immunity. Thus, our findings suggest that adaptive V γ 4 T cells provide dynamic anti-infectious immunity that is subverted by direct translocation of YopJ.

A number of studies have highlighted the importance of IFN γ production from conventional CD4 and CD8 T cells, NK cells, and ILC3 for *Yersinia* resistance [40,43,113,114], although the *in vivo* relevance of Yop inhibition of conventional T cells has not been addressed. Foodborne infection with Yop^{C172A} *Y. pseudotuberculosis* led to an enhanced response from V γ 4 T cells, including increased IFN γ production, that was associated with a more rapid recovery of weight. As IL-12 was critical for V γ 4 T cell derived IFN γ production *in vitro*, the role of IL-12 after foodborne infection of Balb/c mice was assessed. Consistent with previous studies [22,40,115,116], IL-12 appeared critical for protection against foodborne WT and Yop^{C172A} *Y. pseudotuberculosis* infection. As serum IL-12 was only readily detectable after Yop^{C172A} *Y. pseudotuberculosis* infection, increased IL-12 may also contribute to the enhanced IFN γ response from V γ 4 T cells *in vivo*. Finally, assessment of cell populations targeted for Yop translocation *in vivo* was comparable to the results from the *ex vivo* MLN cultures. The highest percentage of Yop⁺ cells were among CD11b⁺ cells and V γ 4 T cells. Given the low MOI used in our *ex vivo* studies with the WT *Yptb*- β la reporter and the lack of inhibition observed in V γ 4 T cells that lack Yop effectors from the same culture conditions, it is likely that intrinsic Yop effects on V γ 4 T cells is a mechanism of inhibiting V γ 4 T cell function *in vivo*. Thus, while *Y. pseudotuberculosis* can use $\gamma\delta$ T cell intrinsic mechanisms to subvert the $\gamma\delta$ T cell IFN γ response, multiple mechanisms may be available for *Yersinia spp.* to subvert $\gamma\delta$ T cell functions to aid pathogenesis *in vivo*. As we previously demonstrated that foodborne but not i.v. infection led to adaptive V γ 4 T cell responses [37], our physiologic foodborne *Y. pseudotuberculosis* infection model revealed novel aspects of *Yersinia* pathogenesis and adaptive V γ 4 T cell biology.

In summary, the *Y. pseudotuberculosis* effector YopJ directly inhibits essential anti-effective functions of murine V γ 4 T cells and human V δ 2⁺ T cells. *Y. pseudotuberculosis* targeted V γ 4 T cells in a T3SS- and YadA-dependent process to deliver Yop effectors directly into V γ 4 T cells. *Ex vivo* whole tissue cultures revealed that direct inhibition of V γ 4 T cell function was the major mechanism of V γ 4 T cell subversion. YopJ translocation led to a dramatic reduction in

STAT4 phosphorylation levels and IFN γ production, which is important for protection from *Yersinia*. YopJ also inhibited a broad anti-infective gene signature. Thus, these findings add substantial insight into YopJ effector functions on murine and human $\gamma\delta$ T cells and the pathogenesis of foodborne *Y. pseudotuberculosis* infection.

Materials and methods

Ethics statement

All animal experiments were conducted in accordance with the Stony Brook University Institutional Animal Care and Use Committee and National Institutes of Health guidelines. Blood collection from healthy human donors was approved by the Institutional Review Board at Stony Brook University.

Mice

Female 8–12 week old BALB/cj mice were purchased from the Jackson Laboratory. Mice were euthanized by CO₂ inhalation.

Human studies

Blood was sampled from a total of 6 adult healthy human donors of either gender between the ages of 20 and 40. Studies were designed so no randomization to experimental groups was necessary. Donors provided written informed consent.

Bacteria

Bacteria strains used in this study include: *Y. pseudotuberculosis* on the 32777 background WT strain, WT32777c, YopJ^{C172A}, YopH^{R409A}, Δ YopB, YopE^{R144A}, YopT^{C139A}, Δ YopM, Δ YpkA, Δ YopK, WT *Yptb*- β la, and Δ YopB *Yptb*- β la. *Y. pseudotuberculosis* on the IP2666 background WT strain, Δ YopB, Δ Inv, Δ YadA, Δ Inv Δ YadA, and Δ YopB Δ Inv Δ YadA. See [Table 1](#) for details. All strains were stored in 25% glycerol stocks at -80°C. For stimulations, *Y. pseudotuberculosis* strains were cultured overnight at 28°C and 220 RPM in LB media. The following morning, *Y. pseudotuberculosis* was sub-cultured 1:10 in LB and 50 mM CaCl₂ at 37°C and 220 RPM for approximately 2 hours. Stimulation doses were based on the OD600.

Foodborne *L. monocytogenes* immunization

L. monocytogenes (EGDe strain) expressing a mutation in the internalin A gene (InlA^M) was used for foodborne infection to facilitate epithelial cell invasion [117]. InlA^M *L. monocytogenes* was cultured overnight at 37°C and 220 RPM in BHI media. The following morning, *L. monocytogenes* was sub-cultured 1:10 in BHI at 37°C and 220 RPM for approximately 2 hours. Infection doses were based on the OD600. Mice were food and water deprived for 4 hours. Approximately 0.5 cm³ bread pieces were inoculated with 2x10⁹ CFU *L. monocytogenes* in 50 μ L. Mice were monitored to ensure the inoculated bread was consumed within 1 hour. Mice that did not fully consume bread were removed from the study. Bacterial infection doses were confirmed by plating inoculum on BHI.

Foodborne *Y. pseudotuberculosis* infection

Y. pseudotuberculosis strains ([Table 1](#)) were cultured overnight at 28°C and 220 RPM in LB media. Infection doses were based on the OD600. Mice were food and water deprived for 4 hours. Approximately 0.5 cm³ bread pieces were inoculated with 2-4x10⁷ CFU for WT32777

Y. pseudotuberculosis, $2\text{-}4\times 10^7\text{-}2\text{-}4\times 10^8$ CFU for YopJ^{C172A} *Y. pseudotuberculosis*, or 2×10^9 CFU for WT *Yptb*- β la infection in 50 μ L. Mice were monitored to ensure the inoculated bread was consumed within 1 hour. Mice that did not fully consume bread were removed from the study. Bacterial infection doses were confirmed by plating inoculum on LB.

Single cell preparations, *Y. pseudotuberculosis* stimulations, and flow cytometry

MLN from *L. monocytogenes* immunized mice were harvested 9 days after immunization and mechanically dissociated using a syringe plunger through a 70 μ m cell strainer into a single cell suspension. Cells were resuspended in IMDM (Gibco) supplemented with 10% fetal bovine serum, 0.01 M HEPES, 100 μ M non-essential amino acids (Gibco), 2 mM L-alanyl-L-glutamine dipeptide in 0.85% NaCl or 1x Glutamax (Gibco), and 1 mM sodium pyruvate. Cells were counted using a Vi-CELL Viability Analyzer (Beckman Coulter). Cells were stimulated in 96 well round-bottom tissue culture treated plates with various strains of *Y. pseudotuberculosis* at 1 or 10 MOI (1 MOI for WT or Δ YopB *Yptb*- β la and 10 MOI for all other *Y. pseudotuberculosis* stimulations, unless otherwise indicated) at 37°C/5% CO₂. 100 U/mL of penicillin and 100 μ g/mL of streptomycin were added to cells 2 hours post-stimulation. Cells were stimulated for a total of 24 hours or as indicated. BD GolgiPlug (BD Biosciences) was added 5 hours prior to the end of stimulation. If translocation was assessed, β -lactamase Loading Solutions kit (Invitrogen) was used to load CCF4-AM by incubating CCF4-AM at RT with cells for 1 hour in the dark. Cells were then processed for surface staining via incubation with live/dead stain, antibody, and Fc block (BioXcell) for 20 min in the dark at 4°C. Antibodies used included antibodies specific to CD45, CD3, TCR δ , CD8, CD4, V γ 1.1, V γ 2, CD44, CD27, F4/80, CD11b, MHCII, CD11c, and CD29 (BioLegend). Cells were fixed, permeabilized, and stained with anti-IFN γ , anti-IRF8, or anti-STAT4 using BD Cytofix/Cytoperm kit (BD Biosciences) for intracellular cytokine staining. Functional $\gamma\delta$ T cell analysis was done by stimulation with BD leukocyte activation cocktail (containing PMA, ionomycin, and brefeldin A; BD Pharmingen) for 4 hours prior to staining. Flow cytometry data were acquired using a BD LSRFortessa and analyzed by FlowJo software (BD Biosciences). Cell culture supernatant was analyzed for IL-12p70 using the BioLegend ELISA MAX Deluxe Set Mouse IL-12 (p70) kit per manufacturer instructions.

Human $\gamma\delta$ T cell response

Blood was drawn and collected from healthy human donors in BD Vacutainer sodium heparin tubes (BD Biosciences). Blood was diluted 1:1 with 1x PBS at room temperature. Peripheral blood mononuclear cells (PBMC) were isolated from the buffy coat of Ficoll-paque PLUS gradient centrifugation (GE Healthcare) for 20 min at 1,400 \times g without a brake. PBMC were washed with 1x PBS at room temperature and resuspended in IMDM supplemented with 10% fetal bovine serum, 0.01 M HEPES, 100 μ M Non-essential amino acids (Gibco), 2 mM L-alanyl-L-glutamine dipeptide in 0.85% NaCl or 1x Glutamax (Gibco), and 1 mM sodium pyruvate. *Y. pseudotuberculosis* strains were cultured overnight at 28°C and 220 RPM in LB media the night prior. The following morning, *Y. pseudotuberculosis* was sub-cultured 1:10 in LB and 50 mM CaCl₂ at 37°C and 220 RPM for approximately 2 hours. Stimulation doses were based on the OD600. Cells were counted using a Vi-CELL Viability Analyzer (Beckman Coulter). Cells were stimulated in 96 round-bottom tissue culture treated plates with various strains of *Y. pseudotuberculosis* at 1 MOI at 37°C/5% CO₂. 1x penicillin and streptomycin (100 U/mL penicillin and 100 μ g/mL streptomycin) were added to cells 2 hours post-stimulation. Cells were stimulated for a total of 24 hours or as indicated. BD GolgiPlug (BD Biosciences) was

added 5 hours prior to the end of stimulation. If translocation was assessed, β -lactamase Loading Solutions kit (Invitrogen) was used to load CCF4-AM by incubating CCF4-AM at RT with cells for 1 hour in the dark. Cells were then processed for surface staining via incubation with live/dead stain, antibody, and Fc block (BioXcell) for 20 min in the dark at 4°C. Antibodies used included antibodies specific to V δ 2, CD3, TCR δ , (BioLegend). Cells were fixed, permeabilized, and stained with anti-IFN γ using BD Cytofix/Cytoperm kit (BD Biosciences) for intracellular cytokine staining. Flow cytometry data were acquired using a BD LSRFortessa and analyzed by FlowJo software (BD Biosciences).

Phospho-flow cytometry

After surface staining for flow cytometry, cells were washed and stained for pSTAT4 using a methanol-based approach. Cells were fixed in 4% PFA/1.5% methanol for 30 minutes in the dark at 4°C. Cells were then washed and incubated in methanol in the dark at 20°C for 45 minutes. After washing, cells were stained with anti-pSTAT4 (Y693)-PE (BD Biosciences) and washed once more. Flow cytometry data were acquired using a BD LSRFortessa and analyzed by FlowJo software (BD Biosciences).

Enumeration of *Y. pseudotuberculosis* burden

MLN were crushed and diluted in media prior to plating on LB agar. Total *Y. pseudotuberculosis* burden per organ was calculated.

Sequencing and analysis

Samples were prepared after *Y. pseudotuberculosis* stimulation as described above. Cell preparations were stimulated with 10 MOI of WT or YopJ^{C172A} *Y. pseudotuberculosis* or 1 MOI of WT *Yptb*- β la for 24 hours. 500 V γ 1.1/2⁻ CD44^{hi} CD27⁻ $\gamma\delta$ T cells were flow sorted directly into a tube with NEBNext Cell Lysis Buffer and Murine RNase Inhibitor and processed for RNA sequencing using NEBNext Single Cell/Low Input RNA Library Prep Kit (Illumina). Sequencing was performed at the Cold Spring Harbor Laboratory sequencing core on a NextSeq500. Fastq files were produced as an output of the sequencing files. Fastq were run through FastQC to perform quality control of transcripts prior to alignment. Fastq files were pair-ended aligned to GRCm38/mm10 by way of HISAT2 and output as .BAM files [118]. Raw counts of aligned transcripts were quantified with FeatureCounts [119]. Dimensionality reduction was performed with PCA analysis with the axes PC1 and PC2 in R-studio [120]. To determine differential expression between samples, FeatureCounts raw count matrix was analyzed through DESeq2 with a parametric fitting normalized to the geometric mean of each individual gene across samples [121]. Cutoff values for significance and quality control were a p-value of <0.05 and FDR-value of <0.10, respectively. Significantly differentially expressed genes were visualized on a heatmap with a dendrogram that was clustered through average linkage. The distance measurement on the dendrogram used was through the Euclidean method. Overlapping expressions between gene differential expression sets were filtered with R-studio. Upregulated and downregulated genes from the differential expression analysis were separated with R-studio and these Gene IDs were used for HOMER motif analysis [74]. Parameters of analysis of each gene used were 400bp preceding the initiation site and 100bp after the initiation site. The length of the motifs analyzed was set between 8 and 10.

$\gamma\delta$ T cell purification

$\gamma\delta$ T cells were expanded *in vitro* according to published protocols [122]. The MLN and spleen were isolated and processed into a single cell suspension 9 days post foodborne *L. monocytogenes* infection of Balb/c mice. Red blood cells were lysed with red blood cell lysis buffer or ammonium chloride for 1 minute and cells from the MLN and spleen were combined. $\gamma\delta$ T cells were enriched by negative selection using the following rat IgG primary antibodies from BioLegend: anti-CD4 (clone GK1.5), anti-CD8 α (clone 53–6.7), anti-B220 (clone RA3-6B2), anti-MHC-II (clone M5/114.15.2), and anti-CD11b (clone M1/70). The MACS goat anti-rat IgG kit (Miltenyi Biotec) was used per manufacturer instructions with MACS LD columns and a QuadroMACS magnet. Enriched cells were cultured in 48-well plates coated overnight with 5 $\mu\text{g}/\text{ml}$ anti-TCR δ (clone GL3). Cells were cultured in RPMI 1640 supplemented with 25 mM HEPES (Gibco), 1x glucose (Gibco), 10 g/ml folate (Sigma Aldrich), 1x sodium pyruvate (Gibco), 5×10^5 M 2 beta-mercaptoethanol (Sigma Aldrich), 1x Glutamax (Gibco), 1x penicillin-streptomycin (Gibco), and 10% FBS with 100 U/ml recombinant human IL-2. After 2 days of culture, cells were transferred into new wells with the same culture media to rest for 5 days. Cells were then stimulated with 10 MOI Yop^{C172A} *Y. pseudotuberculosis* with 0.1, 1, or 10 ng/ml of recombinant murine IL-12p70 (Peprotech).

In vivo anti-IL-12p40 antibody treatment and serum collection

On the day of foodborne WT or Yop^{C172A} *Y. pseudotuberculosis* infection and on day 2, 4, and 6 after infection, mice were treated with 0.2 mg of anti-IL-12p40 (clone C17.8; BioLegend) by i.p. injection. Blood was collected via tail vein on day 2, 4, and 6 after infection. Blood was incubated at ambient temperature for 30 minutes before being spun down at 1500G for 10 minutes at 4°C. Serum was isolated and analyzed for IL-12p70 with the BioLegend ELISA MAX Deluxe Set Mouse IL-12 (p70) kit.

Ex vivo anti-IL-12p40 and recombinant IL-12p70 treatments

At the start of *Y. pseudotuberculosis* stimulation of MLN cell suspensions, cultures were treated with 10 $\mu\text{g}/\text{ml}$ anti-IL-12p40 (clone C17.8; BioLegend) for neutralization. In other conditions, recombinant murine IL-12p70 (Peprotech) was added at the start of *Y. pseudotuberculosis* stimulation of MLN cell suspensions at 2, 10, or 50 ng/ml.

Statistical analysis

GraphPad Prism 6 software (GraphPad Software Inc.) was used for statistical analysis. The differences between the means were compared using the statistical analysis described in the associated figure legends. All the data are presented as mean \pm SEM and $p < 0.05$ was considered significant. * $p < 0.05$, ** $p < 0.01$, *** $p < 0.001$, **** $p < 0.0001$.

Supporting information

S1 Data. Excel spreadsheet containing the underlying numerical data for Figs 1A–1C, 2A and 2B, 3A, 5A–5D and 6A–6F. (XLSX)

S1 Fig. Use of the *Yptb*- β la reporter to track Yop translocation. (A) MLN suspensions from *L. monocytogenes* infected mice were stimulated with WT or Δ YopB *Y. pseudotuberculosis* containing a β -lactamase translocation reporter (*Yptb*- β la) for 2 hours and given antibiotics. Cells were loaded with CCF4-AM dye to measure β -lactamase activity. FITC indicates CCF4-AM

loaded cells without translocation (Yop⁻) and BV421 indicates CCF4-AM loaded cells with Yop translocation (Yop⁺). V γ 1.1/2⁻ CD44^{hi} CD27⁻ $\gamma\delta$ T cells were analyzed for Yop translocation 2 hours post stimulation at an MOI of 10. Representative contour plots are displayed. (B) MLN from *L. monocytogenes* infected mice were stimulated with *Yptb*- β la for 2 hours and given antibiotics. Yop translocation was detected as described above. The indicated cell populations were analyzed for Yop translocation 2 hours after stimulation. Representative contour plots are displayed. (C) MLN from *L. monocytogenes* infected mice were stimulated with *Yptb*- β la for 2 hours and given antibiotics. V γ 1.1/2⁻ CD44^{hi} CD27⁻ $\gamma\delta$ T cells were analyzed for Yop translocation 2 hours post stimulation at the indicated MOI and quantified for Yop translocation. Data consists of one experiment with 2–10 mice/group and the graphs depict the mean \pm SEM in (A–C). ****p < 0.0001, ***p < 0.001, and **p < 0.01. A t-test was used for (A), and a repeated measures one-way ANOVA was used for (C). Comparisons were performed to Δ YopB *Y. pseudotuberculosis* in (A) and as depicted in (C). (TIF)

S2 Fig. The majority of V γ 1.1/2⁻ CD44^{hi} CD27⁻ $\gamma\delta$ T cells and $\gamma\delta$ T cells containing Yop express β 1-integrin. (A) MLN from *L. monocytogenes* infected mice were isolated and processed into single cell suspensions. V γ 1.1/2⁻ CD44^{hi} CD27⁻ $\gamma\delta$ T cells, CD4 T cells, and CD8 T cells were analyzed for β 1-integrin expression. (B) MLN suspensions from *L. monocytogenes* infected mice were loaded with CCF4-AM dye and stimulated with 10 MOI WT *Y. pseudotuberculosis* containing a β -lactamase translocation reporter. CCF4-AM dye reports the occurrence of β -lactamase activity and Yop translocation. $\gamma\delta$ T cells that contain Yop (Yop⁺) or do not contain Yop (Yop⁻) were analyzed for β 1-integrin expression 2 hours after stimulation. Representative histogram plots are displayed. Data is pooled from two experiments with a total of 7 mice/group and the graphs depict the mean \pm SEM in (A–C). ****p < 0.0001 and ***p < 0.001. A repeated measures one-way ANOVA was used for (A) and a t-test was used for (B), and. Comparisons were done to adaptive $\gamma\delta$ T cells in (A) and as depicted in (B). (TIF)

S3 Fig. YopJ regulates the transcriptional profile of V γ 1.1/2⁻ CD44^{hi} CD27⁻ $\gamma\delta$ T cells. (A and B) MLN from *L. monocytogenes* infected mice were stimulated with 10 MOI of WT *Y. pseudotuberculosis* (WT) or mutant YopJ *Y. pseudotuberculosis* (YopJ^{C172A}) for 24 hours. Antibiotics were given 2 hours post-stimulation. Five hundred V γ 1.1/2⁻ CD44^{hi} CD27⁻ $\gamma\delta$ T cells from each stimulation were flow sorted and processed for RNA sequencing. The heat map depicts upregulated genes in V γ 1.1/2⁻ CD44^{hi} CD27⁻ $\gamma\delta$ T cells after YopJ^{C172A} *Y. pseudotuberculosis* stimulation and individual genes are listed. (C–E) Genes differentially expressed (downregulated) that overlapped between RNA sequencing analyses as displayed in the Venn diagram in (C) to select for direct effects of YopJ on V γ 1.1/2⁻ CD44^{hi} CD27⁻ $\gamma\delta$ T cells. The heat map depicts downregulated genes in V γ 1.1/2⁻ CD44^{hi} CD27⁻ $\gamma\delta$ T cells from the analysis in (C). Individual genes are listed in (E). Each experiment was performed once with biologic replicates. The cutoff for gene significance was p < 0.05 and FDR < 0.10. (TIF)

S4 Fig. YopJ does not inhibit IL-17A production in V γ 1.1/2⁻ CD44^{hi} CD27⁻ $\gamma\delta$ T cells. MLN cell suspensions from *L. monocytogenes* infected mice were stimulated with 10 MOI of WT, YopJ^{C172A}, or Δ YopB *Y. pseudotuberculosis* for 24 hours. Antibiotics were given 2 hours after stimulation and brefeldin A was added for the last 5–6 hours. V γ 1.1/2⁻ CD44^{hi} CD27⁻ $\gamma\delta$ T cells were analyzed for IL-17A production after stimulation. Representative histograms are displayed. The graph depicts mean \pm SEM and represents two independent experiments with

4 mice per group. A repeated measures one-way ANOVA was used. * $p < 0.05$. (TIF)

S5 Fig. YopJ impacts IFN γ related transcription factor motifs but not STAT4 protein. (A) Homer motif analysis was performed on the RNA sequencing results for the YopJ^{C172A} and WT *Y. pseudotuberculosis* comparison from Fig 5. The panel highlights the top transcription factor motifs of the ETS, SP/KLF, and IRF family of proteins identified in YopJ^{C172A} stimulated V γ 1.1/2⁻ CD44^{hi} CD27⁻ $\gamma\delta$ T cells. (B) MLN from *L. monocytogenes* infected mice were stimulated with 10 MOI of WT, YopJ^{C172A}, or Δ YopB *Y. pseudotuberculosis* for 6 hours. Antibiotics were given 2 hours post-stimulation. V γ 1.1/2⁻ CD44^{hi} CD27⁻ $\gamma\delta$ T cells were analyzed for IRF8 levels with or without anti-IL12p40 neutralizing antibody. The graph depicts the percentage of IRF8 protein expression among V γ 1.1/2⁻ CD44^{hi} CD27⁻ $\gamma\delta$ T cells after WT, YopJ^{C172A}, or Δ YopB *Y. pseudotuberculosis* stimulation. Data depict two pooled experiments with a total of 8 mice/group and represents the mean \pm SEM. (C) The genes from the RNAseq and Homer motif analysis in Figs 4F and 4G and S3B and S5A were compared to an existing STAT4 ChIP-on-chip dataset to identify common genes. Genes from our dataset that were represented in the top 1000 genes of the Chip-on-chip dataset are displayed. (D) STAT4 KO spleens are shown in maroon and WT spleens are shown in black in representative histograms. The graph depicts the MFI of STAT4 protein expression in bulk $\gamma\delta$ T cells. Data depicts one experiment with 4 mice/group and represents the mean \pm SEM. **** $p < 0.0001$, *** $p < 0.001$, ** $p < 0.01$, * $p < 0.05$. A repeated measures one-way ANOVA was used for (B), and a t-test was used for (D). Comparisons were performed as depicted in (B) and to Naïve WT in (D). (TIF)

S6 Fig. IL-12 is insufficient to induce IFN γ and does not readily overcome the inhibition of YopJ. (A) $\gamma\delta$ T cells enriched from the MLN and spleen of *L. monocytogenes* infected mice were expanded with plate bound $\gamma\delta$ TCR antibody for 2 days and rested for 5 days. After expansion, ~ 50% of cells were $\gamma\delta$ T cells, and the majority of those were V γ 4 T cells. The enrichment summary reflects the mean enrichment from 4 samples. Afterwards, $\gamma\delta$ T cells were isolated from cultures and stimulated with YopJ^{C172A} *Y. pseudotuberculosis* with 0.1, 1, or 10 ng/ml IL-12p70 for 24 hours. Antibiotics were added 2 hours after stimulation and brefeldin A was added for the last 5–6 hours. Histograms display IFN γ production from V γ 1.1/2⁻ CD44^{hi} CD27⁻ $\gamma\delta$ T cells under different culture conditions. Data depicts one experiment with 4 mice pooled and split into the indicated stimulation conditions. (B) MLN cell suspensions from *L. monocytogenes* infected mice were stimulated with 10 MOI of WT *Y. pseudotuberculosis* in the presence of 2, 10, or 50 ng/ml IL-12p70 or 10 MOI of YopJ^{C172A} *Y. pseudotuberculosis* for 24 hours. Antibiotics were given 2 hours after stimulation and brefeldin A was added for the last 5–6 hours. V γ 1.1/2⁻ CD44^{hi} CD27⁻ $\gamma\delta$ T cells were analyzed for IFN γ production. Representative histograms of IFN γ production from V γ 1.1/2⁻ CD44^{hi} CD27⁻ $\gamma\delta$ T cells are displayed. The graph depicts mean \pm SEM from one experiment with 4 mice per group * $p < 0.05$. A repeated measures one-way ANOVA was used for comparisons to YopJ^{C172A} *Y. pseudotuberculosis* in (B). (TIF)

S7 Fig. The impact of foodborne infection of mice with *Y. pseudotuberculosis*. (A) Balb/c mice were foodborne infected with the indicated doses of WT or mutant YopJ^{C172A} *Y. pseudotuberculosis* and tissues were analyzed 9 days post-infection. Bacteria burden was quantified from the MLN. Data reflect 3–5 mice per group pooled from 3 independent experiments and the graphs depict the mean \pm SEM. (B) Balb/c mice were foodborne infected with the indicated doses of WT or mutant YopJ^{C172A} *Y. pseudotuberculosis*. Nine days post infection, MLN

suspensions from WT or YopJ^{C172A} *Y. pseudotuberculosis* infected mice were stimulated with PMA/ionomycin and brefeldin A for 4 hours. V γ 1.1/2⁻ CD44^{hi} CD27⁻ $\gamma\delta$ T cells were analyzed for IFN γ production. Representative histograms are displayed and quantified. Data depicts one experiment with 3 mice per group. (C) Balb/c mice were foodborne infected with WT ($2-4 \times 10^7$ CFU) or YopJ^{C172A} *Y. pseudotuberculosis* ($2-4 \times 10^8$ CFU) and treated with 0.2 mg/mouse of anti-IL12p40 on days 0, 2, 4, and 6 post infection. IL-12p70 concentrations were determined from serum at days 2, 4, and 6 post infection. Data represent 2 independent experiments with a total of 9 mice per group. Serum samples were pooled into groups of 3 per experimental condition. (D) Balb/c mice were foodborne infected with 2×10^9 CFU *L. monocytogenes* to elicit a V γ 1.1/2⁻ CD44^{hi} CD27⁻ $\gamma\delta$ T cell population *in vivo*. 30 days post infection, adaptive V γ 1.1/2⁻ CD44^{hi} CD27⁻ $\gamma\delta$ T cells from the MLN of immune mice were analyzed for Yop translocation using the CCF4-AM assay. Representative contour plots are shown. Yop translocation (Yop⁺) among the indicated populations represents background staining as a negative control for Fig 6F. The graph depicts the mean \pm SEM and is pooled from 2 experiments with a total of 4 mice per group. ****p < 0.0001, *p < 0.05. A one-way ANOVA was used for (A), and an unpaired t-test was used for (B). Comparisons were performed to uninfected in (A) and to 5×10^7 WT *Y. pseudotuberculosis* in (B). (TIF)

Author Contributions

Conceptualization: Timothy H. Chu, Camille Khairallah, James B. Bliska, Brian S. Sheridan.

Data curation: Timothy H. Chu, Camille Khairallah, Jason Shieh.

Formal analysis: Timothy H. Chu, Camille Khairallah, Jason Shieh.

Funding acquisition: Brian S. Sheridan.

Investigation: Timothy H. Chu, Camille Khairallah, Rhea Cho, Zhijuan Qiu.

Methodology: Timothy H. Chu, Camille Khairallah, Yue Zhang, Onur Eskioçak, Semir Beyaz, Brian S. Sheridan.

Project administration: Brian S. Sheridan.

Resources: David G. Thanassi, Mark H. Kaplan, Semir Beyaz, Vincent W. Yang, James B. Bliska.

Supervision: Brian S. Sheridan.

Validation: Timothy H. Chu.

Visualization: Timothy H. Chu, Brian S. Sheridan.

Writing – original draft: Timothy H. Chu.

Writing – review & editing: Timothy H. Chu, Camille Khairallah, David G. Thanassi, James B. Bliska, Brian S. Sheridan.

References

1. Barnes PD, Bergman MA, Mecsas J, Isberg RR. Yersinia pseudotuberculosis disseminates directly from a replicating bacterial pool in the intestine. *J Exp Med*. 2006; 203(6):1591–601. Epub 2006/06/07. <https://doi.org/10.1084/jem.20060905> PMID: 16754724; PubMed Central PMCID: PMC2118325.
2. Autenrieth IB, Kempf V, Sprinz T, Preger S, Schnell A. Defense mechanisms in Peyer's patches and mesenteric lymph nodes against Yersinia enterocolitica involve integrins and cytokines. *Infect Immun*.

- 1996; 64(4):1357–68. Epub 1996/04/01. <https://doi.org/10.1128/iai.64.4.1357-1368.1996> PMID: 8606101; PubMed Central PMCID: PMC173926.
3. Titball RW, Leary SE. Plague. *Br Med Bull.* 1998; 54(3):625–33. Epub 1999/05/18. <https://doi.org/10.1093/oxfordjournals.bmb.a011715> PMID: 10326289.
 4. Hinnebusch BJ. Bubonic plague: a molecular genetic case history of the emergence of an infectious disease. *J Mol Med (Berl).* 1997; 75(9):645–52. Epub 1997/11/14. <https://doi.org/10.1007/s001090050148> PMID: 9351703.
 5. Titball RW, Williamson ED. Vaccination against bubonic and pneumonic plague. *Vaccine.* 2001; 19(30):4175–84. Epub 2001/07/18. [https://doi.org/10.1016/s0264-410x\(01\)00163-3](https://doi.org/10.1016/s0264-410x(01)00163-3) PMID: 11457543.
 6. Inglesby TV, Dennis DT, Henderson DA, Bartlett JG, Ascher MS, Eitzen E, et al. Plague as a biological weapon: medical and public health management. Working Group on Civilian Biodefense. *JAMA.* 2000; 283(17):2281–90. Epub 2000/05/12. <https://doi.org/10.1001/jama.283.17.2281> PMID: 10807389.
 7. Nakajima R, Brubaker RR. Association between virulence of *Yersinia pestis* and suppression of gamma interferon and tumor necrosis factor alpha. *Infect Immun.* 1993; 61(1):23–31. Epub 1993/01/01. <https://doi.org/10.1128/iai.61.1.23-31.1993> PMID: 8418045; PubMed Central PMCID: PMC302683.
 8. Cornelis GR, Boland A, Boyd AP, Geuijen C, Iriarte M, Neyt C, et al. The virulence plasmid of *Yersinia*, an antihost genome. *Microbiol Mol Biol Rev.* 1998; 62(4):1315–52. Epub 1998/12/05. <https://doi.org/10.1128/MMBR.62.4.1315-1352.1998> PMID: 9841674; PubMed Central PMCID: PMC98948.
 9. Cornelis GR, Wolf-Watz H. The *Yersinia* Yop virulon: a bacterial system for subverting eukaryotic cells. *Mol Microbiol.* 1997; 23(5):861–7. Epub 1997/03/01. <https://doi.org/10.1046/j.1365-2958.1997.2731623.x> PMID: 9076724.
 10. Koberle M, Klein-Gunther A, Schutz M, Fritz M, Berchtold S, Tolosa E, et al. *Yersinia enterocolitica* targets cells of the innate and adaptive immune system by injection of Yops in a mouse infection model. *PLoS Pathog.* 2009; 5(8):e1000551. Epub 2009/08/15. <https://doi.org/10.1371/journal.ppat.1000551> PMID: 19680448; PubMed Central PMCID: PMC2718809.
 11. Maldonado-Arocho FJ, Green C, Fisher ML, Paczosa MK, Meccas J. Adhesins and host serum factors drive Yop translocation by *Yersinia* into professional phagocytes during animal infection. *PLoS Pathog.* 2013; 9(6):e1003415. Epub 2013/07/03. <https://doi.org/10.1371/journal.ppat.1003415> PMID: 23818844; PubMed Central PMCID: PMC3688556.
 12. Durand EA, Maldonado-Arocho FJ, Castillo C, Walsh RL, Meccas J. The presence of professional phagocytes dictates the number of host cells targeted for Yop translocation during infection. *Cell Microbiol.* 2010; 12(8):1064–82. Epub 2010/02/13. <https://doi.org/10.1111/j.1462-5822.2010.01451.x> PMID: 20148898; PubMed Central PMCID: PMC2906667.
 13. Viboud GI, Bliska JB. *Yersinia* outer proteins: role in modulation of host cell signaling responses and pathogenesis. *Annu Rev Microbiol.* 2005; 59:69–89. Epub 2005/04/26. <https://doi.org/10.1146/annurev.micro.59.030804.121320> PMID: 15847602.
 14. Cornelis GR. *Yersinia* type III secretion: send in the effectors. *J Cell Biol.* 2002; 158(3):401–8. Epub 2002/08/07. <https://doi.org/10.1083/jcb.200205077> PMID: 12163464; PubMed Central PMCID: PMC2173816.
 15. Bliska JB. *Yersinia* inhibits host signaling by acetylating MAPK kinases. *ACS Chem Biol.* 2006; 1(6):349–51. Epub 2006/12/14. <https://doi.org/10.1021/cb600261k> PMID: 17163770.
 16. Sweet CR, Conlon J, Golenbock DT, Goguen J, Silverman N. YopJ targets TRAF proteins to inhibit TLR-mediated NF-kappaB, MAPK and IRF3 signal transduction. *Cell Microbiol.* 2007; 9(11):2700–15. Epub 2007/07/05. <https://doi.org/10.1111/j.1462-5822.2007.00990.x> PMID: 17608743.
 17. Cao Y, Guan K, He X, Wei C, Zheng Z, Zhang Y, et al. *Yersinia* YopJ negatively regulates IRF3-mediated antibacterial response through disruption of STING-mediated cytosolic DNA signaling. *Biochim Biophys Acta.* 2016; 1863(12):3148–59. Epub 2016/11/05. <https://doi.org/10.1016/j.bbamcr.2016.10.004> PMID: 27742471.
 18. Mukherjee S, Orth K. In vitro signaling by MAPK and NFkappaB pathways inhibited by *Yersinia* YopJ. *Methods Enzymol.* 2008; 438:343–53. Epub 2008/04/17. [https://doi.org/10.1016/S0076-6879\(07\)38024-5](https://doi.org/10.1016/S0076-6879(07)38024-5) PMID: 18413260; PubMed Central PMCID: PMC3432501.
 19. Ma KW, Ma W. YopJ Family Effectors Promote Bacterial Infection through a Unique Acetyltransferase Activity. *Microbiol Mol Biol Rev.* 2016; 80(4):1011–27. Epub 2016/10/28. <https://doi.org/10.1128/MMBR.00032-16> PMID: 27784797; PubMed Central PMCID: PMC5116873.
 20. Orning P, Weng D, Starheim K, Ratner D, Best Z, Lee B, et al. Pathogen blockade of TAK1 triggers caspase-8-dependent cleavage of gasdermin D and cell death. *Science.* 2018; 362(6418):1064–9. Epub 2018/10/27. <https://doi.org/10.1126/science.aau2818> PMID: 30361383; PubMed Central PMCID: PMC6522129.
 21. Rosadini CV, Zaroni I, Odendall C, Green ER, Paczosa MK, Philip NH, et al. A Single Bacterial Immune Evasion Strategy Dismantles Both MyD88 and TRIF Signaling Pathways Downstream of

- TLR4. *Cell Host Microbe*. 2015; 18(6):682–93. Epub 2015/12/15. <https://doi.org/10.1016/j.chom.2015.11.006> PMID: 26651944; PubMed Central PMCID: PMC4685476.
22. Trulzsch K, Geginat G, Sporleder T, Ruckdeschel K, Hoffmann R, Heesemann J, et al. Yersinia outer protein P inhibits CD8 T cell priming in the mouse infection model. *J Immunol*. 2005; 174(7):4244–51. Epub 2005/03/22. <https://doi.org/10.4049/jimmunol.174.7.4244> PMID: 15778387.
 23. Alonso A, Bottini N, Bruckner S, Rahmouni S, Williams S, Schoenberger SP, et al. Lck dephosphorylation at Tyr-394 and inhibition of T cell antigen receptor signaling by Yersinia phosphatase YopH. *J Biol Chem*. 2004; 279(6):4922–8. Epub 2003/11/19. <https://doi.org/10.1074/jbc.M308978200> PMID: 14623872.
 24. Bruckner S, Rhamouni S, Tautz L, Denault JB, Alonso A, Becattini B, et al. Yersinia phosphatase induces mitochondrially dependent apoptosis of T cells. *J Biol Chem*. 2005; 280(11):10388–94. Epub 2005/01/06. <https://doi.org/10.1074/jbc.M408829200> PMID: 15632192.
 25. Yao T, Meccas J, Healy JI, Falkow S, Chien Y. Suppression of T and B lymphocyte activation by a Yersinia pseudotuberculosis virulence factor, yopH. *J Exp Med*. 1999; 190(9):1343–50. Epub 1999/11/02. <https://doi.org/10.1084/jem.190.9.1343> PMID: 10544205; PubMed Central PMCID: PMC2195683.
 26. Gerke C, Falkow S, Chien YH. The adaptor molecules LAT and SLP-76 are specifically targeted by Yersinia to inhibit T cell activation. *J Exp Med*. 2005; 201(3):361–71. Epub 2005/02/09. <https://doi.org/10.1084/jem.20041120> PMID: 15699071; PubMed Central PMCID: PMC2213036.
 27. Viney J, MacDonald TT, Spencer J. Gamma/delta T cells in the gut epithelium. *Gut*. 1990; 31(8):841–4. Epub 1990/08/01. <https://doi.org/10.1136/gut.31.8.841> PMID: 2143741; PubMed Central PMCID: PMC1378605.
 28. Goodman T, Lefrancois L. Expression of the gamma-delta T-cell receptor on intestinal CD8+ intraepithelial lymphocytes. *Nature*. 1988; 333(6176):855–8. Epub 1988/06/30. <https://doi.org/10.1038/333855a0> PMID: 2968521.
 29. Ribeiro ST, Ribot JC, Silva-Santos B. Five Layers of Receptor Signaling in gammadelta T-Cell Differentiation and Activation. *Front Immunol*. 2015; 6:15. Epub 2015/02/13. <https://doi.org/10.3389/fimmu.2015.00015> PMID: 25674089; PubMed Central PMCID: PMC4306313.
 30. Yin Z, Zhang DH, Welte T, Bahtiyar G, Jung S, Liu L, et al. Dominance of IL-12 over IL-4 in gamma delta T cell differentiation leads to default production of IFN-gamma: failure to down-regulate IL-12 receptor beta 2-chain expression. *J Immunol*. 2000; 164(6):3056–64. Epub 2000/03/08. <https://doi.org/10.4049/jimmunol.164.6.3056> PMID: 10706694.
 31. Li W, Kubo S, Okuda A, Yamamoto H, Ueda H, Tanaka T, et al. Effect of IL-18 on expansion of gammadelta T cells stimulated by zoledronate and IL-2. *J Immunother*. 2010; 33(3):287–96. Epub 2010/05/07. <https://doi.org/10.1097/CJI.0b013e3181c80ffa> PMID: 20445349.
 32. Moens E, Brouwer M, Dimova T, Goldman M, Willems F, Vermijlen D. IL-23R and TCR signaling drives the generation of neonatal Vgamma9Vdelta2 T cells expressing high levels of cytotoxic mediators and producing IFN-gamma and IL-17. *J Leukoc Biol*. 2011; 89(5):743–52. Epub 2011/02/19. <https://doi.org/10.1189/jlb.0910501> PMID: 21330350.
 33. Sutton CE, Lalor SJ, Sweeney CM, Brereton CF, Lavelle EC, Mills KH. Interleukin-1 and IL-23 induce innate IL-17 production from gammadelta T cells, amplifying Th17 responses and autoimmunity. *Immunity*. 2009; 31(2):331–41. Epub 2009/08/18. <https://doi.org/10.1016/j.immuni.2009.08.001> PMID: 19682929.
 34. Lockhart E, Green AM, Flynn JL. IL-17 production is dominated by gammadelta T cells rather than CD4 T cells during Mycobacterium tuberculosis infection. *J Immunol*. 2006; 177(7):4662–9. Epub 2006/09/20. <https://doi.org/10.4049/jimmunol.177.7.4662> PMID: 16982905.
 35. Ribot JC, Chaves-Ferreira M, d'Orey F, Wencker M, Goncalves-Sousa N, Decalf J, et al. Cutting edge: adaptive versus innate receptor signals selectively control the pool sizes of murine IFN-gamma- or IL-17-producing gammadelta T cells upon infection. *J Immunol*. 2010; 185(11):6421–5. Epub 2010/11/03. <https://doi.org/10.4049/jimmunol.1002283> PMID: 21037088; PubMed Central PMCID: PMC3915338.
 36. Garman RD, Doherty PJ, Raulet DH. Diversity, rearrangement, and expression of murine T cell gamma genes. *Cell*. 1986; 45(5):733–42. Epub 1986/06/06. [https://doi.org/10.1016/0092-8674\(86\)90787-7](https://doi.org/10.1016/0092-8674(86)90787-7) PMID: 3486721.
 37. Sheridan BS, Romagnoli PA, Pham QM, Fu HH, Alonzo F, 3rd, Schubert WD, et al. gammadelta T cells exhibit multifunctional and protective memory in intestinal tissues. *Immunity*. 2013; 39(1):184–95. Epub 2013/07/31. <https://doi.org/10.1016/j.immuni.2013.06.015> PMID: 23890071; PubMed Central PMCID: PMC3749916.
 38. Romagnoli PA, Sheridan BS, Pham QM, Lefrancois L, Khanna KM. IL-17A-producing resident memory gammadelta T cells orchestrate the innate immune response to secondary oral Listeria monocytogenes infection. *Proc Natl Acad Sci U S A*. 2016; 113(30):8502–7. Epub 2016/07/13. <https://doi.org/10.1073/pnas.1600713113> PMID: 27402748; PubMed Central PMCID: PMC4968747.

39. Dillen CA, Pinsker BL, Marusina AI, Merleev AA, Farber ON, Liu H, et al. Clonally expanded gamma-delta T cells protect against Staphylococcus aureus skin reinfection. *J Clin Invest*. 2018; 128(3):1026–42. Epub 2018/02/06. <https://doi.org/10.1172/JCI96481> PMID: 29400698; PubMed Central PMCID: PMC5824877.
40. Bohn E, Autenrieth IB. IL-12 is essential for resistance against Yersinia enterocolitica by triggering IFN-gamma production in NK cells and CD4+ T cells. *J Immunol*. 1996; 156(4):1458–68. Epub 1996/02/15. PMID: 8568248.
41. Szaba FM, Kummer LW, Duso DK, Koroleva EP, Tumanov AV, Cooper AM, et al. TNFalpha and IFN-gamma but not perforin are critical for CD8 T cell-mediated protection against pulmonary Yersinia pestis infection. *PLoS Pathog*. 2014; 10(5):e1004142. Epub 2014/05/24. <https://doi.org/10.1371/journal.ppat.1004142> PMID: 24854422; PubMed Central PMCID: PMC4031182.
42. Logsdon LK, Meccas J. The proinflammatory response induced by wild-type Yersinia pseudotuberculosis infection inhibits survival of yop mutants in the gastrointestinal tract and Peyer's patches. *Infect Immun*. 2006; 74(3):1516–27. Epub 2006/02/24. <https://doi.org/10.1128/IAI.74.3.1516-1527.2006> PMID: 16495522; PubMed Central PMCID: PMC1418670.
43. Seo GY, Shui JW, Takahashi D, Song C, Wang Q, Kim K, et al. LIGHT-HVEM Signaling in Innate Lymphoid Cell Subsets Protects Against Enteric Bacterial Infection. *Cell Host Microbe*. 2018; 24(2):249–60 e4. Epub 2018/08/10. <https://doi.org/10.1016/j.chom.2018.07.008> PMID: 30092201; PubMed Central PMCID: PMC6132068.
44. Imperato JN, Xu D, Romagnoli PA, Qiu Z, Perez P, Khairallah C, et al. Mucosal CD8 T Cell Responses Are Shaped by Batf3-DC After Foodborne Listeria monocytogenes Infection. *Front Immunol*. 2020; 11:575967. Epub 2020/10/13. <https://doi.org/10.3389/fimmu.2020.575967> PMID: 33042159; PubMed Central PMCID: PMC7518468.
45. Zhang Y, Murtha J, Roberts MA, Siegel RM, Bliska JB. Type III secretion decreases bacterial and host survival following phagocytosis of Yersinia pseudotuberculosis by macrophages. *Infect Immun*. 2008; 76(9):4299–310. Epub 2008/07/02. <https://doi.org/10.1128/IAI.00183-08> PMID: 18591234; PubMed Central PMCID: PMC2519449.
46. Palmer LE, Hobbie S, Galan JE, Bliska JB. YopJ of Yersinia pseudotuberculosis is required for the inhibition of macrophage TNF-alpha production and downregulation of the MAP kinases p38 and JNK. *Mol Microbiol*. 1998; 27(5):953–65. Epub 1998/04/16. <https://doi.org/10.1046/j.1365-2958.1998.00740.x> PMID: 9535085.
47. Simonet M, Falkow S. Invasin expression in Yersinia pseudotuberculosis. *Infect Immun*. 1992; 60(10):4414–7. Epub 1992/10/01. <https://doi.org/10.1128/iai.60.10.4414-4417.1992> PMID: 1398952; PubMed Central PMCID: PMC257481.
48. Ivanov MI, Stuckey JA, Schubert HL, Saper MA, Bliska JB. Two substrate-targeting sites in the Yersinia protein tyrosine phosphatase co-operate to promote bacterial virulence. *Mol Microbiol*. 2005; 55(5):1346–56. Epub 2005/02/22. <https://doi.org/10.1111/j.1365-2958.2005.04477.x> PMID: 15720545.
49. Bliska JB, Guan KL, Dixon JE, Falkow S. Tyrosine phosphate hydrolysis of host proteins by an essential Yersinia virulence determinant. *Proc Natl Acad Sci U S A*. 1991; 88(4):1187–91. Epub 1991/02/15. <https://doi.org/10.1073/pnas.88.4.1187> PMID: 1705028; PubMed Central PMCID: PMC50982.
50. McPhee JB, Mena P, Bliska JB. Delineation of regions of the Yersinia YopM protein required for interaction with the RSK1 and PRK2 host kinases and their requirement for interleukin-10 production and virulence. *Infect Immun*. 2010; 78(8):3529–39. Epub 2010/06/03. <https://doi.org/10.1128/IAI.00269-10> PMID: 20515922; PubMed Central PMCID: PMC2916259.
51. Schoberle TJ, Chung LK, McPhee JB, Bogin B, Bliska JB. Uncovering an Important Role for YopJ in the Inhibition of Caspase-1 in Activated Macrophages and Promoting Yersinia pseudotuberculosis Virulence. *Infect Immun*. 2016; 84(4):1062–72. Epub 2016/01/27. <https://doi.org/10.1128/IAI.00843-15> PMID: 26810037; PubMed Central PMCID: PMC4807483.
52. Chung LK, Philip NH, Schmidt VA, Koller A, Strowig T, Flavell RA, et al. IQGAP1 is important for activation of caspase-1 in macrophages and is targeted by Yersinia pestis type III effector YopM. *mBio*. 2014; 5(4):e01402–14. Epub 2014/07/06. <https://doi.org/10.1128/mBio.01402-14> PMID: 24987096; PubMed Central PMCID: PMC4161239.
53. Harmon DE, Davis AJ, Castillo C, Meccas J. Identification and characterization of small-molecule inhibitors of Yop translocation in Yersinia pseudotuberculosis. *Antimicrob Agents Chemother*. 2010; 54(8):3241–54. Epub 2010/05/26. <https://doi.org/10.1128/AAC.00364-10> PMID: 20498321; PubMed Central PMCID: PMC2916352.
54. Schweer J, Kulkarni D, Kochut A, Pezoldt J, Pisano F, Pils MC, et al. The cytotoxic necrotizing factor of Yersinia pseudotuberculosis (CNFY) enhances inflammation and Yop delivery during infection by activation of Rho GTPases. *PLoS Pathog*. 2013; 9(11):e1003746. Epub 2013/11/19. <https://doi.org/10.1371/journal.ppat.1003746> PMID: 24244167; PubMed Central PMCID: PMC3820761.

55. Zhang Y, Tam JW, Mena P, van der Velden AW, Bliska JB. CCR2+ Inflammatory Dendritic Cells and Translocation of Antigen by Type III Secretion Are Required for the Exceptionally Large CD8+ T Cell Response to the Protective YopE69-77 Epitope during Yersinia Infection. *PLoS Pathog.* 2015; 11(10): e1005167. Epub 2015/10/16. <https://doi.org/10.1371/journal.ppat.1005167> PMID: 26468944; PubMed Central PMCID: PMC4607306.
56. Zhang Y, Romanov G, Bliska JB. Type III secretion system-dependent translocation of ectopically expressed Yop effectors into macrophages by intracellular Yersinia pseudotuberculosis. *Infect Immun.* 2011; 79(11):4322–31. Epub 2011/08/17. <https://doi.org/10.1128/IAI.05396-11> PMID: 21844228; PubMed Central PMCID: PMC3257923.
57. Kim J, Fukuto HS, Brown DA, Bliska JB, London E. Effects of host cell sterol composition upon internalization of Yersinia pseudotuberculosis and clustered beta1 integrin. *J Biol Chem.* 2018; 293(4):1466–79. Epub 2017/12/05. <https://doi.org/10.1074/jbc.M117.811224> PMID: 29197826; PubMed Central PMCID: PMC5787820.
58. Bohn E, Sonnabend M, Klein K, Autenrieth IB. Bacterial adhesion and host cell factors leading to effector protein injection by type III secretion system. *Int J Med Microbiol.* 2019; 309(5):344–50. Epub 2019/06/11. <https://doi.org/10.1016/j.ijmm.2019.05.008> PMID: 31178419.
59. Isberg RR, Voorhis DL, Falkow S. Identification of invasins: a protein that allows enteric bacteria to penetrate cultured mammalian cells. *Cell.* 1987; 50(5):769–78. Epub 1987/08/28. [https://doi.org/10.1016/0092-8674\(87\)90335-7](https://doi.org/10.1016/0092-8674(87)90335-7) PMID: 3304658.
60. Schulze-Koops H, Burkhardt H, Heesemann J, von der Mark K, Emmrich F. Plasmid-encoded outer membrane protein YadA mediates specific binding of enteropathogenic yersiniae to various types of collagen. *Infect Immun.* 1992; 60(6):2153–9. Epub 1992/06/01. <https://doi.org/10.1128/iai.60.6.2153-2159.1992> PMID: 1587583; PubMed Central PMCID: PMC257137.
61. Deuschle E, Keller B, Siegfried A, Manncke B, Spaeth T, Koberle M, et al. Role of beta1 integrins and bacterial adhesins for Yop injection into leukocytes in Yersinia enterocolitica systemic mouse infection. *Int J Med Microbiol.* 2016; 306(2):77–88. Epub 2016/01/01. <https://doi.org/10.1016/j.ijmm.2015.12.001> PMID: 26718660.
62. Bliska JB, Copass MC, Falkow S. The Yersinia pseudotuberculosis adhesin YadA mediates intimate bacterial attachment to and entry into HEp-2 cells. *Infect Immun.* 1993; 61(9):3914–21. Epub 1993/09/01. <https://doi.org/10.1128/iai.61.9.3914-3921.1993> PMID: 7689542; PubMed Central PMCID: PMC281094.
63. Nguyen GT, McCabe AL, Fasciano AC, Meccas J. Detection of Cells Translocated with Yersinia Yops in Infected Tissues Using beta-Lactamase Fusions. *Methods Mol Biol.* 2019; 2010:117–39. Epub 2019/06/10. https://doi.org/10.1007/978-1-4939-9541-7_9 PMID: 31177435; PubMed Central PMCID: PMC6733027.
64. Pasztoi M, Bonifacius A, Pezoldt J, Kulkarni D, Niemz J, Yang J, et al. Yersinia pseudotuberculosis supports Th17 differentiation and limits de novo regulatory T cell induction by directly interfering with T cell receptor signaling. *Cell Mol Life Sci.* 2017; 74(15):2839–50. Epub 2017/04/06. <https://doi.org/10.1007/s00018-017-2516-y> PMID: 28378044; PubMed Central PMCID: PMC5491567.
65. Elfiky A, Bonifacius A, Pezoldt J, Pasztoi M, Chaoprasid P, Sadana P, et al. Yersinia Pseudotuberculosis Modulates Regulatory T Cell Stability via Injection of Yersinia Outer Proteins in a Type III Secretion System-Dependent Manner. *Eur J Microbiol Immunol (Bp).* 2018; 8(4):101–6. Epub 2019/02/06. <https://doi.org/10.1556/1886.2018.00015> PMID: 30719325; PubMed Central PMCID: PMC6348704.
66. Clark MA, Hirst BH, Jepson MA. M-cell surface beta1 integrin expression and invasins-mediated targeting of Yersinia pseudotuberculosis to mouse Peyer's patch M cells. *Infect Immun.* 1998; 66(3):1237–43. Epub 1998/03/06. <https://doi.org/10.1128/IAI.66.3.1237-1243.1998> PMID: 9488419; PubMed Central PMCID: PMC108039.
67. El Tahir Y, Skurnik M. YadA, the multifaceted Yersinia adhesin. *Int J Med Microbiol.* 2001; 291(3):209–18. Epub 2001/09/14. <https://doi.org/10.1078/1438-4221-00119> PMID: 11554561.
68. Terti R, Skurnik M, Vartio T, Kuusela P. Adhesion protein YadA of Yersinia species mediates binding of bacteria to fibronectin. *Infect Immun.* 1992; 60(7):3021–4. Epub 1992/07/01. <https://doi.org/10.1128/iai.60.7.3021-3024.1992> PMID: 1612772; PubMed Central PMCID: PMC257272.
69. Flugel A, Schulze-Koops H, Heesemann J, Kuhn K, Sorokin L, Burkhardt H, et al. Interaction of enteropathogenic Yersinia enterocolitica with complex basement membranes and the extracellular matrix proteins collagen type IV, laminin-1 and -2, and nidogen/entactin. *J Biol Chem.* 1994; 269(47):29732–8. Epub 1994/11/25. PMID: 7961965.
70. Mukherjee S, Keitany G, Li Y, Wang Y, Ball HL, Goldsmith EJ, et al. Yersinia YopJ acetylates and inhibits kinase activation by blocking phosphorylation. *Science.* 2006; 312(5777):1211–4. Epub 2006/05/27. <https://doi.org/10.1126/science.1126867> PMID: 16728640.
71. Lee J, Aoki T, Thumkeo D, Siritwach R, Yao C, Narumiya S. T cell-intrinsic prostaglandin E2-EP2/EP4 signaling is critical in pathogenic TH17 cell-driven inflammation. *J Allergy Clin Immunol.* 2019; 143

- (2):631–43. Epub 2018/06/24. <https://doi.org/10.1016/j.jaci.2018.05.036> PMID: 29935220; PubMed Central PMCID: PMC6354914.
72. Ng SS, De Labastida Rivera F, Yan J, Corvino D, Das I, Zhang P, et al. The NK cell granule protein NKG7 regulates cytotoxic granule exocytosis and inflammation. *Nat Immunol.* 2020; 21(10):1205–18. Epub 2020/08/26. <https://doi.org/10.1038/s41590-020-0758-6> PMID: 32839608.
73. Malarkannan S. NKG7 makes a better killer. *Nat Immunol.* 2020; 21(10):1139–40. Epub 2020/08/26. <https://doi.org/10.1038/s41590-020-0767-5> PMID: 32839609.
74. Heinz S, Benner C, Spann N, Bertolino E, Lin YC, Laslo P, et al. Simple combinations of lineage-determining transcription factors prime cis-regulatory elements required for macrophage and B cell identities. *Mol Cell.* 2010; 38(4):576–89. Epub 2010/06/02. <https://doi.org/10.1016/j.molcel.2010.05.004> PMID: 20513432; PubMed Central PMCID: PMC2898526.
75. Pham D, Sehra S, Sun X, Kaplan MH. The transcription factor Ets1 controls TH17 cell development and allergic airway inflammation. *J Allergy Clin Immunol.* 2014; 134(1):204–14. Epub 2014/02/04. <https://doi.org/10.1016/j.jaci.2013.12.021> PMID: 24486067; PubMed Central PMCID: PMC4209254.
76. Yin L, Li W, Xu A, Shi H, Wang K, Yang H, et al. SH3BGR2 inhibits growth and metastasis in clear cell renal cell carcinoma via activating hippo/TEAD1-Twist1 pathway. *EBioMedicine.* 2020; 51:102596. Epub 2020/01/09. <https://doi.org/10.1016/j.ebiom.2019.12.005> PMID: 31911271; PubMed Central PMCID: PMC7000347.
77. Pham D, Vincentz JW, Firulli AB, Kaplan MH. Twist1 regulates Ifng expression in Th1 cells by interfering with Runx3 function. *J Immunol.* 2012; 189(2):832–40. Epub 2012/06/12. <https://doi.org/10.4049/jimmunol.1200854> PMID: 22685315; PubMed Central PMCID: PMC3392532.
78. Wang Y, Godec J, Ben-Aissa K, Cui K, Zhao K, Pucsek AB, et al. The transcription factors T-bet and Runx are required for the ontogeny of pathogenic interferon-gamma-producing T helper 17 cells. *Immunity.* 2014; 40(3):355–66. Epub 2014/02/18. <https://doi.org/10.1016/j.immuni.2014.01.002> PMID: 24530058; PubMed Central PMCID: PMC3965587.
79. Good SR, Thieu VT, Mathur AN, Yu Q, Stritesky GL, Yeh N, et al. Temporal induction pattern of STAT4 target genes defines potential for Th1 lineage-specific programming. *J Immunol.* 2009; 183(6):3839–47. Epub 2009/08/28. <https://doi.org/10.4049/jimmunol.0901411> PMID: 19710469; PubMed Central PMCID: PMC2748807.
80. Xu X, Sun YL, Hoey T. Cooperative DNA binding and sequence-selective recognition conferred by the STAT amino-terminal domain. *Science.* 1996; 273(5276):794–7. Epub 1996/08/09. <https://doi.org/10.1126/science.273.5276.794> PMID: 8670419.
81. Yamamoto K, Miura O, Hirose S, Miyasaka N. Binding sequence of STAT4: STAT4 complex recognizes the IFN-gamma activation site (GAS)-like sequence (T/A)TTCC(C/G)GGAA(T/A). *Biochem Biophys Res Commun.* 1997; 233(1):126–32. Epub 1997/04/07. <https://doi.org/10.1006/bbrc.1997.6415> PMID: 9144409.
82. Zhang Y, Ting AT, Marcu KB, Bliska JB. Inhibition of MAPK and NF-kappa B pathways is necessary for rapid apoptosis in macrophages infected with Yersinia. *J Immunol.* 2005; 174(12):7939–49. Epub 2005/06/10. <https://doi.org/10.4049/jimmunol.174.12.7939> PMID: 15944300.
83. Khairallah C, Bettke JA, Gorbatshevych O, Qiu Z, Zhang Y, Cho K, et al. A blend of broadly-reactive and pathogen-selected Vgamma4 Vdelta1 T cell receptors confer broad bacterial reactivity of resident memory gammadelta T cells. *Mucosal Immunol.* 2021. Epub 2021/09/01. <https://doi.org/10.1038/s41385-021-00447-x> PMID: 34462572.
84. Young JL, Goodall JC, Beacock-Sharp H, Gaston JS. Human gamma delta T-cell recognition of Yersinia enterocolitica. *Immunology.* 1997; 91(4):503–10. Epub 1997/08/01. <https://doi.org/10.1046/j.1365-2567.1997.00289.x> PMID: 9378487; PubMed Central PMCID: PMC1363868.
85. Hermann E, Ackermann B, Duchmann R, Meyer zum Buschenfelde KH. Synovial fluid MHC-unrestricted gamma delta-T lymphocytes contribute to antibacterial and anti-self cytotoxicity in the spondylarthropathies. *Clin Exp Rheumatol.* 1995; 13(2):187–91. Epub 1995/03/01. PMID: 7656464.
86. Huang D, Chen CY, Ali Z, Shao L, Shen L, Lockman HA, et al. Antigen-specific Vgamma2Vdelta2 T effector cells confer homeostatic protection against pneumonic plaque lesions. *Proc Natl Acad Sci U S A.* 2009; 106(18):7553–8. Epub 2009/04/23. <https://doi.org/10.1073/pnas.0811250106> PMID: 19383786; PubMed Central PMCID: PMC2678605.
87. Puan KJ, Jin C, Wang H, Sarikonda G, Raker AM, Lee HK, et al. Preferential recognition of a microbial metabolite by human Vgamma2Vdelta2 T cells. *Int Immunol.* 2007; 19(5):657–73. Epub 2007/04/21. <https://doi.org/10.1093/intimm/dxm031> PMID: 17446209.
88. Hermann E, Lohse AW, Mayet WJ, van der Zee R, Van Eden W, Probst P, et al. Stimulation of synovial fluid mononuclear cells with the human 65-kD heat shock protein or with live enterobacteria leads to preferential expansion of TCR-gamma delta+ lymphocytes. *Clin Exp Immunol.* 1992; 89(3):427–33.

- Epub 1992/09/01. <https://doi.org/10.1111/j.1365-2249.1992.tb06975.x> PMID: 1387595; PubMed Central PMCID: PMC1554482.
89. Deseke M, Prinz I. Ligand recognition by the gammadelta TCR and discrimination between homeostasis and stress conditions. *Cell Mol Immunol*. 2020; 17(9):914–24. Epub 2020/07/28. <https://doi.org/10.1038/s41423-020-0503-y> PMID: 32709926.
 90. Cui W, Joshi NS, Jiang A, Kaech SM. Effects of Signal 3 during CD8 T cell priming: Bystander production of IL-12 enhances effector T cell expansion but promotes terminal differentiation. *Vaccine*. 2009; 27(15):2177–87. Epub 2009/02/10. <https://doi.org/10.1016/j.vaccine.2009.01.088> PMID: 19201385; PubMed Central PMCID: PMC2803112.
 91. Robinson RT, Khader SA, Locksley RM, Lien E, Smiley ST, Cooper AM. Yersinia pestis evades TLR4-dependent induction of IL-12(p40)₂ by dendritic cells and subsequent cell migration. *J Immunol*. 2008; 181(8):5560–7. Epub 2008/10/04. <https://doi.org/10.4049/jimmunol.181.8.5560> PMID: 18832714; PubMed Central PMCID: PMC2640496.
 92. Koch I, Dach K, Heesemann J, Hoffmann R. Yersinia enterocolitica inactivates NK cells. *Int J Med Microbiol*. 2013; 303(8):433–42. Epub 2013/07/03. <https://doi.org/10.1016/j.ijmm.2013.05.004> PMID: 23810728.
 93. Garcia VE, Jullien D, Song M, Uyemura K, Shuai K, Morita CT, et al. IL-15 enhances the response of human gamma delta T cells to nonpeptide [correction of nonpetide] microbial antigens. *J Immunol*. 1998; 160(9):4322–9. Epub 1998/05/09. PMID: 9574535.
 94. Orth K. Function of the Yersinia effector YopJ. *Curr Opin Microbiol*. 2002; 5(1):38–43. Epub 2002/02/09. [https://doi.org/10.1016/s1369-5274\(02\)00283-7](https://doi.org/10.1016/s1369-5274(02)00283-7) PMID: 11834367.
 95. Li C, Wang D, Lv X, Jing R, Bi B, Chen X, et al. Yersinia pestis acetyltransferase-mediated dual acetylation at the serine and lysine residues enhances the auto-ubiquitination of ubiquitin ligase MARCH8 in human cells. *Cell Cycle*. 2017; 16(7):649–59. Epub 2017/01/20. <https://doi.org/10.1080/15384101.2017.1281481> PMID: 28103160; PubMed Central PMCID: PMC5397269.
 96. Zhou H, Monack DM, Kayagaki N, Wertz I, Yin J, Wolf B, et al. Yersinia virulence factor YopJ acts as a deubiquitinase to inhibit NF-kappa B activation. *J Exp Med*. 2005; 202(10):1327–32. Epub 2005/11/23. <https://doi.org/10.1084/jem.20051194> PMID: 16301742; PubMed Central PMCID: PMC2212976.
 97. Keller B, Muhlenkamp M, Deuschle E, Siegfried A, Mossner S, Schade J, et al. Yersinia enterocolitica exploits different pathways to accomplish adhesion and toxin injection into host cells. *Cell Microbiol*. 2015; 17(8):1179–204. Epub 2015/02/14. <https://doi.org/10.1111/cmi.12429> PMID: 25678064.
 98. Morinobu A, Gadina M, Strober W, Visconti R, Fornace A, Montagna C, et al. STAT4 serine phosphorylation is critical for IL-12-induced IFN-gamma production but not for cell proliferation. *Proc Natl Acad Sci U S A*. 2002; 99(19):12281–6. Epub 2002/09/06. <https://doi.org/10.1073/pnas.182618999> PMID: 12213961; PubMed Central PMCID: PMC129436.
 99. Mavropoulos A, Sully G, Cope AP, Clark AR. Stabilization of IFN-gamma mRNA by MAPK p38 in IL-12- and IL-18-stimulated human NK cells. *Blood*. 2005; 105(1):282–8. Epub 2004/09/04. <https://doi.org/10.1182/blood-2004-07-2782> PMID: 15345584.
 100. Zhang W, Liu HT. MAPK signal pathways in the regulation of cell proliferation in mammalian cells. *Cell Res*. 2002; 12(1):9–18. Epub 2002/04/11. <https://doi.org/10.1038/sj.cr.7290105> PMID: 11942415.
 101. Gehart H, Kumpf S, Ittner A, Ricci R. MAPK signalling in cellular metabolism: stress or wellness? *EMBO Rep*. 2010; 11(11):834–40. Epub 2010/10/12. <https://doi.org/10.1038/embor.2010.160> PMID: 20930846; PubMed Central PMCID: PMC2966959.
 102. Wilkinson MG, Millar JB. Control of the eukaryotic cell cycle by MAP kinase signaling pathways. *FASEB J*. 2000; 14(14):2147–57. Epub 2000/10/29. <https://doi.org/10.1096/fj.00-0102rev> PMID: 11053235.
 103. Sugiura R, Satoh R, Ishiwata S, Umeda N, Kita A. Role of RNA-Binding Proteins in MAPK Signal Transduction Pathway. *J Signal Transduct*. 2011; 2011:109746. Epub 2011/07/22. <https://doi.org/10.1155/2011/109746> PMID: 21776382; PubMed Central PMCID: PMC3135068.
 104. Kopper F, Bierwirth C, Schon M, Kunze M, Elvers I, Kranz D, et al. Damage-induced DNA replication stalling relies on MAPK-activated protein kinase 2 activity. *Proc Natl Acad Sci U S A*. 2013; 110(42):16856–61. Epub 2013/10/02. <https://doi.org/10.1073/pnas.1304355110> PMID: 24082115; PubMed Central PMCID: PMC3801042.
 105. Wei JH, Seemann J. Remodeling of the Golgi structure by ERK signaling. *Commun Integr Biol*. 2009; 2(1):35–6. Epub 2009/08/26. <https://doi.org/10.4161/cib.2.1.7421> PMID: 19704864; PubMed Central PMCID: PMC2649298.
 106. Grenningloh R, Kang BY, Ho IC. Ets-1, a functional cofactor of T-bet, is essential for Th1 inflammatory responses. *J Exp Med*. 2005; 201(4):615–26. Epub 2005/02/25. <https://doi.org/10.1084/jem.20041330> PMID: 15728239; PubMed Central PMCID: PMC2213045.

107. Koues OI, Collins PL, Cella M, Robinette ML, Porter SI, Pyfrom SC, et al. Distinct Gene Regulatory Pathways for Human Innate versus Adaptive Lymphoid Cells. *Cell*. 2016; 165(5):1134–46. Epub 2016/05/10. <https://doi.org/10.1016/j.cell.2016.04.014> PMID: 27156452; PubMed Central PMCID: PMC4874868.
108. Dandekar AA, O'Malley K, Perlman S. Important roles for gamma interferon and NKG2D in gamma-delta T-cell-induced demyelination in T-cell receptor beta-deficient mice infected with a coronavirus. *J Virol*. 2005; 79(15):9388–96. Epub 2005/07/15. <https://doi.org/10.1128/JVI.79.15.9388-9396.2005> PMID: 16014902; PubMed Central PMCID: PMC1181615.
109. Nitahara A, Shimura H, Ito A, Tomiyama K, Ito M, Kawai K. NKG2D ligation without T cell receptor engagement triggers both cytotoxicity and cytokine production in dendritic epidermal T cells. *J Invest Dermatol*. 2006; 126(5):1052–8. Epub 2006/02/18. <https://doi.org/10.1038/sj.jid.5700112> PMID: 16484989.
110. Girardi M, Oppenheim DE, Steele CR, Lewis JM, Glusac E, Filler R, et al. Regulation of cutaneous malignancy by gammadelta T cells. *Science*. 2001; 294(5542):605–9. Epub 2001/09/22. <https://doi.org/10.1126/science.1063916> PMID: 11567106
111. Osinska I, Popko K, Demkow U. Perforin: an important player in immune response. *Cent Eur J Immunol*. 2014; 39(1):109–15. Epub 2014/01/01. <https://doi.org/10.5114/cej.2014.42135> PMID: 26155110; PubMed Central PMCID: PMC4439970.
112. Gogoi D, Chiplunkar SV. Targeting gamma delta T cells for cancer immunotherapy: bench to bedside. *Indian J Med Res*. 2013; 138(5):755–61. Epub 2014/01/18. PMID: 24434328; PubMed Central PMCID: PMC3928706.
113. Autenrieth IB, Beer M, Bohn E, Kaufmann SH, Heesemann J. Immune responses to Yersinia enterocolitica in susceptible BALB/c and resistant C57BL/6 mice: an essential role for gamma interferon. *Infect Immun*. 1994; 62(6):2590–9. Epub 1994/06/01. <https://doi.org/10.1128/iai.62.6.2590-2599.1994> PMID: 8188382; PubMed Central PMCID: PMC186549.
114. Bohn E, Heesemann J, Ehlers S, Autenrieth IB. Early gamma interferon mRNA expression is associated with resistance of mice against Yersinia enterocolitica. *Infect Immun*. 1994; 62(7):3027–32. Epub 1994/07/01. <https://doi.org/10.1128/iai.62.7.3027-3032.1994> PMID: 8005693; PubMed Central PMCID: PMC302917.
115. Hein J, Sing A, Di Genaro MS, Autenrieth IB. Interleukin-12 and interleukin-18 are indispensable for protective immunity against enteropathogenic Yersinia. *Microb Pathog*. 2001; 31(4):195–9. Epub 2001/09/20. <https://doi.org/10.1006/mpat.2001.0458> PMID: 11562172.
116. Bohn E, Schmitt E, Bielfeldt C, Noll A, Schulte R, Autenrieth IB. Ambiguous role of interleukin-12 in Yersinia enterocolitica infection in susceptible and resistant mouse strains. *Infect Immun*. 1998; 66(5):2213–20. Epub 1998/05/09. <https://doi.org/10.1128/IAI.66.5.2213-2220.1998> PMID: 9573110; PubMed Central PMCID: PMC108184.
117. Wollert T, Pasche B, Rochon M, Deppenmeier S, van den Heuvel J, Gruber AD, et al. Extending the host range of Listeria monocytogenes by rational protein design. *Cell*. 2007; 129(5):891–902. Epub 2007/06/02. <https://doi.org/10.1016/j.cell.2007.03.049> PMID: 17540170.
118. Kim D, Langmead B, Salzberg SL. HISAT: a fast spliced aligner with low memory requirements. *Nat Methods*. 2015; 12(4):357–60. Epub 2015/03/10. <https://doi.org/10.1038/nmeth.3317> PMID: 25751142; PubMed Central PMCID: PMC4655817.
119. Liao Y, Smyth GK, Shi W. featureCounts: an efficient general purpose program for assigning sequence reads to genomic features. *Bioinformatics*. 2014; 30(7):923–30. Epub 2013/11/15. <https://doi.org/10.1093/bioinformatics/btt656> PMID: 24227677.
120. Stacklies W, Redestig H, Scholz M, Walther D, Selbig J. pcaMethods—a bioconductor package providing PCA methods for incomplete data. *Bioinformatics*. 2007; 23(9):1164–7. Epub 2007/03/09. <https://doi.org/10.1093/bioinformatics/btm069> PMID: 17344241.
121. Love MI, Huber W, Anders S. Moderated estimation of fold change and dispersion for RNA-seq data with DESeq2. *Genome Biol*. 2014; 15(12):550. Epub 2014/12/18. <https://doi.org/10.1186/s13059-014-0550-8> PMID: 25516281; PubMed Central PMCID: PMC4302049.
122. Collins C, Shi C, Russell JQ, Fortner KA, Budd RC. Activation of gamma delta T cells by Borrelia burgdorferi is indirect via a TLR- and caspase-dependent pathway. *J Immunol*. 2008; 181(4):2392–8. Epub 2008/08/08. <https://doi.org/10.4049/jimmunol.181.4.2392> PMID: 18684928; PubMed Central PMCID: PMC2832482.